Biochem. J. (2010) **430**, 49–59 (Printed in Great Britain) doi:10.1042/BJ20100633

online data

Identification of S-nitrosated mitochondrial proteins by *S*-nitrosothiol difference in gel electrophoresis (SNO-DIGE): implications for the regulation of mitochondrial function by reversible S-nitrosation

Edward T. CHOUCHANI*, Thomas R. HURD*, Sergiy M. NADTOCHIY†, Paul S. BROOKES†, Ian M. FEARNLEY*, Kathryn S. LILLEY‡, Robin A. J. SMITH§ and Michael P. MURPHY*[1]

*MRC Mitochondrial Biology Unit, Hills Road, Cambridge CB2 0XY, U.K., †Department of Anesthesiology, University of Rochester Medical Center, 601 Elmwood Avenue, Rochester, NY 14642, U.S.A., ‡Department of Biochemistry, Cambridge System Biology Centre, University of Cambridge, Cambridge CB2 1GA, U.K., and §Department of Chemistry, University of Otago, P.O. Box 56, Dunedin 9054, New Zealand

The S-nitrosation of mitochondrial proteins as a consequence of NO metabolism is of physiological and pathological significance. We previously developed a MitoSNO (mitochondria-targeted *S*-nitrosothiol) that selectively S-nitrosates mitochondrial proteins. To identify these S-nitrosated proteins, here we have developed a selective proteomic methodology, SNO-DIGE (*S*-nitrosothiol difference in gel electrophoresis). Protein thiols in control and MitoSNO-treated samples were blocked, then incubated with copper(II) and ascorbate to selectively reduce *S*-nitrosothiols. The samples were then treated with thiol-reactive Cy3 (indocarbocyanine) or Cy5 (indodicarbocyanine) fluorescent tags, mixed together and individual protein spots were resolved by 2D (two-dimensional) gel electrophoresis. Fluorescent scanning of these gels revealed S-nitrosated proteins by an increase in Cy5 red fluorescence, allowing for their identification by MS. Parallel analysis by Redox-DIGE enabled us to distinguish S-nitrosated thiol proteins from those which became oxidized due to NO metabolism. We identified 13 S-nitrosated mitochondrial proteins, and a further four that were oxidized, probably due to evanescent S-nitrosation relaxing to a reversible thiol modification. We investigated the consequences of S-nitrosation for three of the enzymes identified using SNO-DIGE (aconitase, mitochondrial aldehyde dehydrogenase and α-ketoglutarate dehydrogenase) and found that their activity was selectively and reversibly inhibited by S-nitrosation. We conclude that the reversible regulation of enzyme activity by S-nitrosation modifies enzymes central to mitochondrial metabolism, whereas identification and functional characterization of these novel targets provides mechanistic insight into the potential physiological and pathological roles played by this modification. More generally, the development of SNO-DIGE facilitates robust investigation of protein S-nitrosation across the proteome.

Key words: difference in gel electrophoresis (DIGE), mitochondria, nitric oxide (NO), redox signalling, S-nitrosation, S-nitrosylation.

INTRODUCTION

Reversible S-nitrosation affects a number of mitochondrial proteins and is thought to be a major way in which NO metabolism modulates mitochondrial physiology and pathology [1,2]. Within cells, mitochondria are exposed to significant concentrations of NO from NOSs (nitric oxide synthases), resulting in substantial effects on mitochondrial respiration [3]. Although some mechanisms of NO action have been established, such as its reversible active site inhibition of cytochrome *c* oxidase, the breadth of protein targets of NO within mitochondria is not well understood. In particular, the pathways by which NO metabolism leads to protein S-nitrosation and the physiological consequences of these modifications remain obscure [4,5]. Previous work has identified complex I as an important site of mitochondrial S-nitrosation and, although this modification is known to affect its activity [2,6], a number of additional mitochondrial proteins are also S-nitrosated [6,7]. Despite this, the identities of these additional targets and their functional responses to S-nitrosation are poorly understood. Consequently, there is still considerable uncertainty regarding the majority of mitochondrial proteins affected by S-nitrosation and the functional consequences of these modifications.

To investigate mitochondrial S-nitrosation, we developed a MitoSNO (mitochondria-targeted *S*-nitrosothiol) that rapidly accumulates several-hundred fold within energized mitochondria, leading to the selective S-nitrosation of mitochondrial protein thiols (Figure 1) [6]. MitoSNO consists of the well-characterized NO donor SNAP (*S*-nitroso-*N*-acetylpenicillamine) conjugated to a lipophilic TPP (triphenylphosphonium) cationic moiety. The delocalized positive charge and lipophilic surface of TPP allows MitoSNO to rapidly cross biological membranes and to accumulate several hundred-fold within energized mitochondria *in vivo*, driven by membrane potential across the mitochondrial inner membrane. The local pH and reducing conditions then allow for the selective transnitrosation of protein thiols sensitive to S-nitrosation within mitochondria. We previously found that MitoSNO only S-nitrosated a small proportion (~1%)

Abbreviations used: 2D, two-dimensional; ALDH2, aldehyde dehydrogenase; AR, area at risk; BVA, biological variance analysis; Cy3, indocarbocyanine; Cy5, indodicarbocyanine; DIGE, difference in gel electrophoresis; DTT, dithiothreitol; GSNO, *S*-nitrosoglutathione; I/R, ischaemia/reperfusion; α-KGDH, α-ketoglutarate dehydrogenase; LAD, left anterior descending coronary artery; LV, left ventricle; MALDI–TOF-TOF, matrix-assisted laser-desorption ionization–time-of-flight time-of-flight; MitoNAP, mito-*N*-acetylpenicillamine; MitoSNO, mitochondria-targeted *S*-nitrosothiol; NEM, *N*-ethylmaleimide; NIH, National Institutes for Health; PrSNO, protein *S*-nitrosothiol; RHM, rat heart mitochondria; RLM, rat liver mitochondria; ROS, reactive oxygen species; SA, standardized abundance; SNAP, *S*-nitroso-*N*-acetylpenicillamine; SNO-DIGE, *S*-nitrosothiol difference in gel electrophoresis; TPP, triphenylphosphonium.

[1] To whom correspondence should be addressed (email mpm@mrc-mbu.cam.ac.uk).

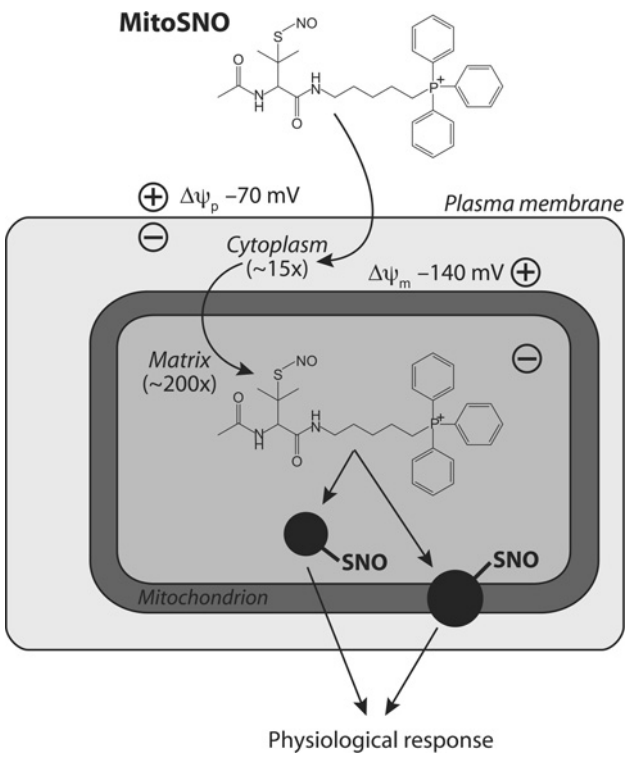

Figure 1 S-nitrosation of mitochondrial proteins by MitoSNO

According to the Nernst equation, lipophilic triphenylphosphonium cations accumulate approx. 10-fold for every 60 mV of membrane potential ($\Delta\psi$). With approximate values of $\Delta\psi$ in the heart being 70 mV across the plasma membrane and 140 mV across the mitochondrial inner membrane, these potential differences lead to an approx. 3000-fold accumulation of MitoSNO within mitochondria. MitoSNO will S-nitrosate mitochondrial thiol proteins by transferring a nitrosonium group (NO^+) to protein thiolates.

of the mitochondrial protein thiols available, and these thiols were present on a limited subset of mitochondrial proteins [6]. These results suggest that the mitochondrial proteins S-nitrosated by MitoSNO are those that are particularly susceptible to S-nitrosation and are therefore candidates for the potential consequent physiological response. Therefore identifying these targets should open new insights into the physiological and pathological roles of mitochondrial S-nitrosation.

Here we set out to identify those mitochondrial proteins, in addition to complex I, that are susceptible to S-nitrosation. To do this we developed a selective proteomic technique based on the DIGE (difference in gel electrophoresis) method [8]. This approach, which we called SNO-DIGE (*S*-nitrosothiol DIGE), allowed us to identify proteins containing thiols sensitive to S-nitrosation selectively. SNO-DIGE is an extension of a technique we previously developed, Redox-DIGE, which we used to identify mitochondrial protein thiols sensitive to ROS (reactive oxygen species) [9,10]. The SNO-DIGE method provides significant improvements in sensitivity over previous proteomic screens for these low-abundance targets of S-nitrosation. By making use of a highly selective reduction of protein *S*-nitrosothiols [11] in a proteomic study we overcome the insufficient and non-specific reduction conditions used in previous screens. Additionally, by incorporating controls for biological variability into the experimental design, we significantly improved the statistical power of the method [12,13]. Therefore using SNO-DIGE, we identified a number of mitochondrial proteins that are novel targets of reversible S-nitrosation. By investigating the functional consequences of these modifications, we provide mechanistic insights into mitochondrial protein S-nitrosation and its potential contribution to mitochondrial physiology and pathology.

MATERIALS AND METHODS

Chemical syntheses

MitoSNO and MitoNAP (mito-*N*-acetylpenicillamine) were synthesized as described previously [6]. Solutions were stored in absolute ethanol at −80 °C. MitoSNO stability was assessed prior to use from its absorbance at 340 nm.

Mitochondrial preparations and incubations

RHM (rat heart mitochondria) and RLM (rat liver mitochondria) were prepared as described previously, by homogenization of tissue in STE (250 mM sucrose, 5 mM Tris/HCl and 1 mM EGTA, pH 7.4), supplemented with 0.1 % fatty-acid-free BSA for the heart, followed by differential centrifugation [14]. Protein concentrations were measured by the biuret assay using BSA as a standard [15].

Sample preparation for PrSNO (protein *S*-nitrosothiol) reduction control experiments

RHM (2 mg protein) were incubated with 10 mM succinate and 4 μg/ml rotenone to generate significant mitochondrial respiration, membrane potential and negligible superoxide production, with or without 10 μM MitoSNO for 5 min at 37 °C in 250 mM sucrose, 5 mM Hepes, 1 mM EGTA and 10 μM neocuproine. Following incubation, 50 mM NEM (*N*-ethyl maleimide) was added and the protein samples were pelleted. Pellets were resuspended in an assay medium containing 10 mM Hepes, 1 mM EGTA, 100 μM neocuproine and 50 mM NEM, pH 7.4, and incubated for 5 min at 37 °C prior to the addition of 1 % SDS and incubation for a further 5 min. NEM was removed from the samples by passing them through three Micro Bio-Spin 6 chromatography columns (Bio-Rad), while maintaining a 1 % SDS concentration. Specific reduction and labelling of protein *S*-nitrosothiols was achieved by addition of 1 mM ascorbate and 10 μM $CuSO_4$ in Chelex 100-treated PBS buffer, pH 7.5, in the presence of 200 μM Cy3 (indocarbocyanine)-maleimide (GE Healthcare). When UV photolysis was used to degrade PrSNOs either before the addition of NEM or instead of copper(II) and ascorbate reduction, samples were exposed to UV irradiation at 355 nm at room temperature (23 °C) for either 2 or 5 min. Incubation with the fluorescent maleimide proceeded for 30 min at 37 °C. The protein (20 μg) was then separated on SDS/PAGE (12.5 % gel). After electrophoresis, the gel image was acquired with a Typhoon 9410 variable mode imager.

Sample preparation for SNO-DIGE and Redox-DIGE

RHM (2 mg of protein) were incubated as above, with or without 10 μM MitoSNO for 5 min at 37 °C. Following incubation, 50 mM NEM was added and the protein samples were pelleted. Pellets were resuspended in an NEM-containing assay medium as described above and incubated for 5 min at 37 °C prior to the addition of 1 % SDS and incubation for a further 5 min. NEM was removed from the samples by passing them through three Micro Bio-Spin 6 chromatography columns (Bio-Rad), maintaining a 1 % SDS concentration throughout. Specific reduction of *S*-nitrosothiols in the samples was achieved by addition of 1 mM ascorbate and 10 μM $CuSO_4$ in Chelex 100-treated PBS buffer in the presence of 40 μM CyDye™ DIGE Fluor Cy™3 saturation

dye (Cy3) or CyDye™ DIGE Fluor Cy™5 saturation dye [Cy5 (indodicarbocyanine)] (GE Healthcare). After 30 min at 37 °C, the excess CyDye™ reactivity was quenched with 2.5 mM DTT (dithiothreitol) and the samples were snap frozen on dry ice prior to pooling and resolution by 2D (two-dimensional) electrophoresis. Protein samples for Redox-DIGE were treated as above, except that for reduction samples were treated with 2.5 mM DTT for 10 min at room temperature, instead of copper(II) and ascorbate, prior to removal of DTT using two column chromatography steps followed by reaction with Cy3 or Cy5 [9,10].

DIGE experimental design

To assess differences in fluorescence using DIGE, sample pooling on the basis of BVA (biological variance analysis) was employed. Each DIGE experiment used three biological replicates from independently prepared mitochondria. One fluorescent component of each gel (in this case Cy3) comprised a pooled standard of equal amounts of protein from each biological replicate, and the Cy5 component of each gel was an individual treatment (either control or MitoSNO treated) [13]. Each DIGE analysis therefore consisted of six gels from three biological replicates, where three compared the control condition to the pooled standard and three compared the MitoSNO-treated condition to the pooled standard.

Electrophoresis, gel imaging and analysis

Resolution of mitochondrial proteins by 2D gel electrophoresis was carried out as described previously [9]. Gels were transferred on to a Typhoon™ 9410 imager (GE Healthcare). Cy3 fluorescent images were obtained using a 532 nm laser and a 580 nm emission filter (band pass 30 nm). Cy5 fluorescent images were obtained using a 633 nm laser and a 670 nm emission filter (band pass 30 nm). All gels were scanned at 100 μm pixel size, and the photomultiplier tube was set to ensure a maximum pixel intensity within the range of 40000 and 80000. Analysis of the 2D fluorescent images was performed using the DeCyder™ BVA module version 6.5 (GE Healthcare), a 2D gel analysis software package designed specifically for DIGE. The software was used following the manufacturer's recommendations. Briefly, the estimated number of spots was set to 2500 per gel, and each protein spot across six gel images was matched automatically, then checked and matched manually. Successfully matched spots were compared across groups according to SA (standardized abundance), where a sample spot fluorescence volume (Cy5) is divided by the standard spot volume (Cy3), normalized with ratiometric normalization and transformed with a $\log_{10}$ function. Comparing SA, differences across the two groups were considered significant at >2, $P < 0.05$.

Spot excision and MS

For MS of proteins from the DIGE analysis, 400 μg of fluorescently tagged protein was separated by 2D gel electrophoresis and the fluorescent image was matched to the gels used for image analysis. Then the gel was stained with Coomassie Blue for spot excision. Coomassie Blue-stained images were scanned and spot matched to overlaid fluorescent images to ensure accurate excision of proteins of interest. Protein spots were digested by 'in-gel' cleavage [16] at 37 °C with 12.5 ng/ml sequencing grade trypsin (Roche Applied Science) in 20 mM Tris/HCl, pH 8.0, and 5 mM $CaCl_2$. Peptides were extracted from the gel with 4 % ARISTAR-grade formic acid and 60 % acetonitrile solution. All digests were analysed in a model 4800 MALDI–TOF-TOF (matrix-assisted laser-desorption ionization–time-of-flight time-of-flight) mass spectrometer (Applied Biosystems) using α-cyano-hydroxy-*trans*-cinnamic acid as the matrix. The instrument was calibrated with bovine trypsin autolysis products (*m/z* values 2163.057 and 2273.160) and a calcium-related matrix ion (*m/z* value 1060.048). Peptide masses and peptide fragmentation data were searched against the NCBI (National Center for Biotechnology Information) database *Rattus* entries with a peptide tolerance of $\pm$ 25 p.p.m., tandem MS tolerance of $\pm$ 0.8 Da and permitted missed cleavages of 1 [17].

Mitochondrial incubations for enzyme assays

RHM or RLM (2 mg of protein) were incubated with 10 mM succinate and 4 μg/ml rotenone, with 10 μM MitoSNO, 10 μM MitoNAP or no additions in a 120 mM KCl solution containing 1 mM EDTA, 1 mM DTPA (diethylenetriaminepenta-acetic acid) and 10 μM neocuproine, pH 7.4, at 37 °C. At the indicated time points, aliquots were removed and snap frozen on dry ice. To reverse S-nitrosation, samples were incubated for 15 min at room temperature in assay buffer containing 0.1 % Triton X-100 supplemented with 10 μM $CuSO_4$ and 1 mM ascorbate. To reverse thiol oxidation, samples were incubated for 10 min at room temperature in assay buffer containing 0.1 % Triton X-100 supplemented with 1 mM DTT.

Mitochondrial enzyme activity assays

Mitochondrial aconitase activity was measured spectrophotometrically by a coupled enzyme assay [18]. Protein (25 μg) was added to 50 mM Tris/HCl, pH 7.4, 0.6 mM $MnCl_2$, 5 mM sodium citrate and 0.1 % Triton X-100. After equilibration at 30 °C, 0.2 mM $NADP^+$ and 0.4 unit/ml isocitrate dehydrogenase were added and the initial linear change in A_{340} was measured. The activity of α-KGDH (α-ketoglutarate dehydrogenase) was measured spectrophotometrically [19]. Protein (75 μg) was added to 50 mM potassium phosphate buffer, pH 7.4, 0.2 mM EGTA, 0.2 mM thiamine pyrophosphate, 2 mM NAD^+, 1 mM $MgCl_2$, 0.4 mM ADP, 10 μM rotenone and 0.1 % Triton X-100. After equilibration at 30 °C, 0.12 mM CoA and 1 mM α-ketoglutarate were added and the initial linear change in A_{340} was recorded. Mitochondrial ALDH2 (aldehyde dehydrogenase) activity was also measured spectrophotometrically [20]. For this, 500 μg of protein was added to 60 mM sodium phosphate buffer, pH 7.4, 1 mM EDTA, 1 mM NAD^+ and 1 % Triton X-100 at 25 °C. Then, 1 mM propionaldehyde was added and the initial linear change in A_{340} was recorded.

Mouse heart I/R (ischaemia/reperfusion) experiments

Male C57BL/6 mice ($\sim$25 g) were purchased from the Jackson Laboratory and handled in accordance with a protocol approved by the procedures of the University of Rochester Committee on Animal Research. All protocols were in accordance with the NIH (National Institutes for Health) Guide for the care and use of laboratory animals. All surgical procedures were sterile and performed as described previously [21]. Briefly, analgesics (acetaminophen 0.75 mg/ml in drinking water) were administered 24 h before, and during the perioperative period. Following anaesthesia (Avertin, 2,2,2-tribromoethanol, 0.5 mg/kg intraperitoneally) mice were intubated and connected to a rodent ventilator. A thoracotomy was performed and the LAD (left anterior descending coronary artery) was then ligated and occluded for 30 min. MitoSNO or MitoNAP (100 ng/kg) were

dissolved in 0.9 % NaCl saline (final volume 50μl) and then administered 5 min prior to reperfusion into the LV (left ventricle) using 30G × 0.5 inch needle. Reperfusion was initiated by removing the suture. The chest and skin were sutured closed, the endotracheal tube removed and the animal returned to its cage to recover. After 24 h, the animal was re-anaesthetized, the LAD re-ligated, and Evans' Blue dye (1.0 %, w/v, 1.5 ml) was perfused via the LV. The heart was removed and cut transversely into five sections, which were incubated in 1.0 % 2,3,5-triphenyltetrazolium chloride at 37 °C for 10 min. The AR (area at risk) and infarct zone were indicated by the areas unstained with Evans' Blue and TTC (triphenyltetrazolium chloride) respectively [21]. Slices were scanned and infarct/AR ratios determined with NIH ImageJ software.

RESULTS

The SNO-DIGE method

Previously published work suggested that a small number of heart mitochondrial proteins were S-nitrosated by MitoSNO [6]. To identify these proteins, we developed a novel and sensitive proteomic technique, SNO-DIGE. The development of resolvable fluorescent DIGE dyes allows for comparison of multiple samples on a single 2D gel, greatly enhancing reproducibility and confidence in differences observed across the proteome [8]. Previously, we extended the basic DIGE method by developing Redox-DIGE to identify mitochondrial thiol proteins that are particularly sensitive to reversible oxidation during a redox challenge [9,10]. To do so we made use of cysteine-reactive DIGE dyes [22] to label oxidized protein thiols selectively. In the present study we have further extended the DIGE methodology to identify S-nitrosated proteins selectively (Figure 2). The procedure first relies on blocking exposed thiols with the alkylating agent NEM. Critically, the S-nitrosated thiols are then selectively reduced by copper(I), generated by treatment with ascorbate and copper(II) sulfate [11] in the presence of fluorescent Cy5 maleimide for the S-nitrosated and control samples, or in the presence of fluorescent Cy3 maleimide for the standard samples. Thus the S-nitrosated proteins should contain a Cy5 fluorescent tag, whereas the controls should not. This enables the spots containing the S-nitrosated thiols to be selected and identified by peptide mass fingerprinting and tandem MS.

Previous work by our group and others has demonstrated that copper (II) and ascorbate reduction of thiol proteins is highly efficient and specific for PrSNOs, leaving other reversible thiol modifications intact [6,11]. To further support these findings in the system employed in this study we used UV photolysis, another means of degrading PrSNOs, to establish the specificity of copper (II) and ascorbate reduction conditions (see Supplementary Figure S1 at http://www.BiochemJ.org/bj/430/bj4300049add.htm). Treatment of RHM with MitoSNO followed by NEM blocking of free thiols and reduction of PrSNOs with copper(II) and ascorbate in the presence of a fluorescent maleimide dye resulted in fluorescent tagging of a number of mitochondrial thiol proteins (Supplementary Figure S1, lane 2). Subjecting samples to UV photolysis for 5 min following MitoSNO treatment and prior to NEM blocking resulted in a complete loss of the fluorescent signal under the same reduction conditions (Supplementary Figure S1, lane 4), suggesting that in the presence of copper(II) and ascorbate, fluorescent labelling is exclusively of PrSNOs. In addition, degrading PrSNOs by UV photolysis instead of copper(II) and ascorbate resulted in labelling of virtually the same cohort of proteins (Supplementary Figure S1, lanes 5 and 6 compared with lane 2). These findings support previous work establishing the efficiency and specificity of copper(II) and ascorbate reduction of PrSNOs and further justify the use of these reduction conditions for use with SNO-DIGE.

In carrying out SNO-DIGE, we made the first use in a study of this type of an experimental design based on BVA, which greatly assists in the identification of the small proportion of proteins genuinely S-nitrosated by decreasing the impact of biological variability across replicate experiments [12]. BVA makes use of a pooled standard containing equal amounts of protein from three biological replicates, against which each individual control or S-nitrosated condition is compared. The advantage of this approach is that it accounts for the effects of both biological and technical variation, since the same pooled standard is present in each gel and therefore can be used for inter-gel normalization [10,13,23]. Additionally, because the control and S-nitrosated conditions under comparison both rely on proteins being tagged with the same dye (Cy5 maleimide), dye-specific effects that can manifest as false positives are eliminated [24].

The SNO-DIGE methodology is described in detail in Figure 2. Samples from the same source are either untreated (control and standard, Figures 2A and 2B respectively) or treated with MitoSNO (S-nitrosated, Figure 2C). NEM and SDS are then added to the samples to block all exposed protein thiols. Following the removal of NEM, ascorbate and copper(II) are added to selectively reduce PrSNOs [11]. This PrSNO-specific reduction proceeds in the presence of Cy5 maleimide (false coloured red fluorescence) for both control and treated samples or in the presence of Cy3 maleimide (false coloured green fluorescence) for the standard sample. For each DIGE experiment, samples are prepared from three independent biological samples, following which all Cy3-labelled standard samples are pooled. The normalized combined standard is then mixed individually with each of the three Cy5 MitoSNO-treated samples and each of the three Cy5 control samples. Six Cy3/Cy5 mixtures are then resolved individually by 2D electrophoresis and scanned for Cy3 and Cy5 fluorescence (Figures 2D and 2E). DeCyder™ version 6.5 BVA software (GE Healthcare) was used to match each protein spot and assess the fluorescence differences across the six gels. This enabled the differences between the Cy5 fluorescence of control and S-nitrosated samples to be compared, whereas the pooled standard allowed for robust statistical analysis across gels.

As expected for SNO-DIGE analysis, most proteins were unlabelled by the fluorescent maleimide dyes in both control and treated conditions, consistent with the majority of protein thiols being in a reduced state (Figures 2D and 2E). A small number of proteins appeared as intense yellow spots in both control and S-nitrosated samples, indicating that these proteins were equally labelled under both conditions. This was expected and is due to occluded protein thiols, such as those involved in Fe-S centres, that were unreactive with NEM but subsequently became exposed during sample preparation [9]. We corroborated this by identifying the four most prominent equally tagged proteins by MS (see Supplementary Table S1 at http://www.BiochemJ.org/bj/430/bj4300049add.htm). Those protein spots that were red in the MitoSNO-treated gels (Figures 2E and 3A), but not in the control gels (Figures 2D and 3A), were indicative of S-nitrosated proteins. Thus we were able to resolve and distinguish a number of S-nitrosated protein thiols sensitively using the SNO-DIGE method.

Assessment of oxidized protein thiols by Redox-DIGE

A proportion of the S-nitrosation of mitochondrial proteins by MitoSNO may be transient, relaxing to disulfide bond,

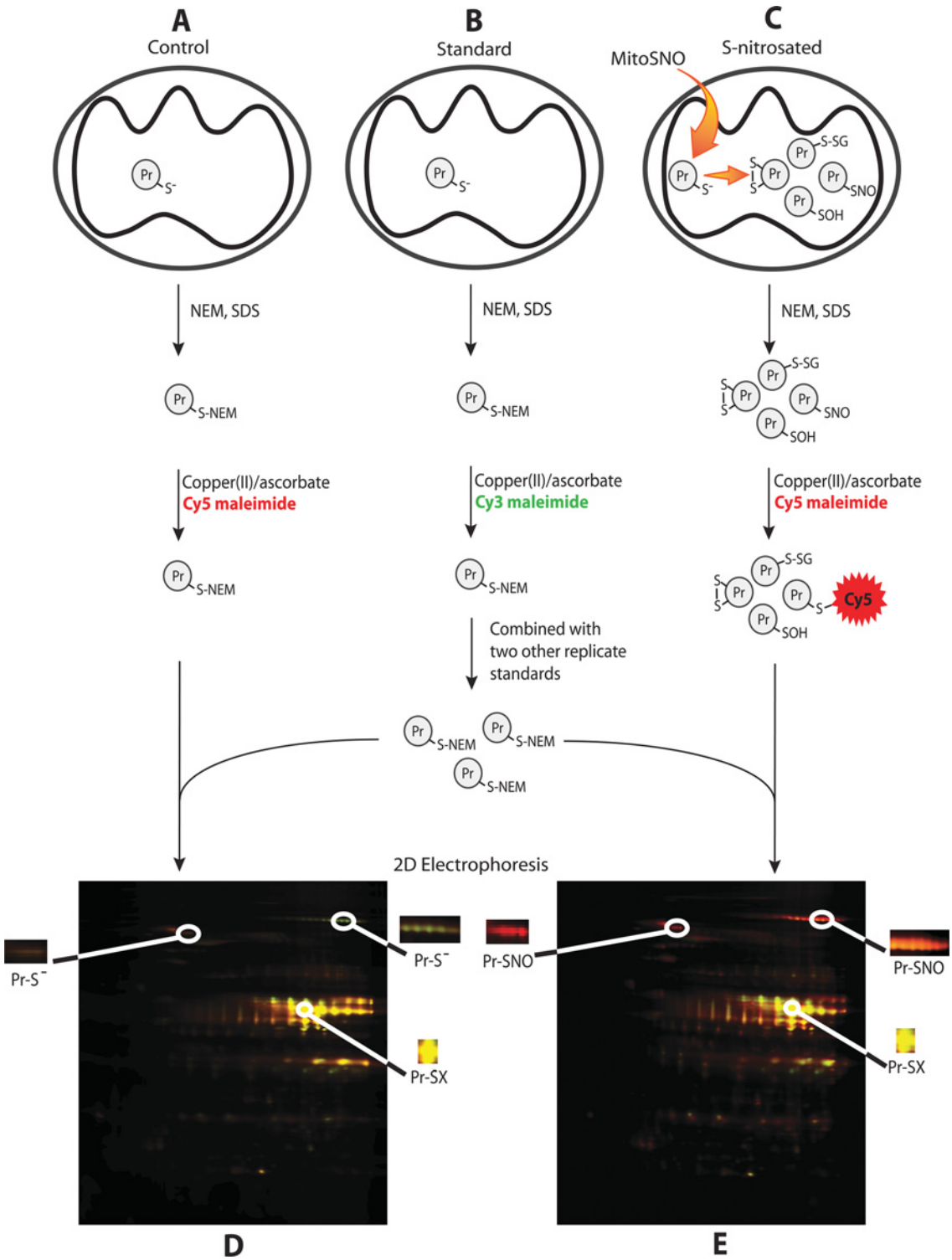

Figure 2 SNO-DIGE experimental design

Protein from the same biological source is divided into three pools for a single replicate experiment: control (**A**), standard (**B**) and S-nitrosated (**C**). In control and standard samples, free protein thiols are blocked with NEM in the presence of SDS, treated with ascorbate and $CuSO_4$, and labelled with Cy5 and Cy3 maleimide (red and green respectively). In S-nitrosated samples treated with MitoSNO (**C**), some protein thiols may become S-nitrosated and unreactive with NEM. S-nitrosated thiols can then be selectively reduced with ascorbate and $CuSO_4$ and tagged with Cy5 maleimide (red), whereas all other oxidative modifications remain untagged. The Cy3-labelled standard sample from a single replicate is pooled with the standard sample from two independent preparations and combined individually with the control and treated Cy5 samples of every replicate sample (three control, three treated; six in total). Combined samples are resolved by 2D electrophoresis on the same gel and scanned for red and green fluorescence. Protein spots that appear red on the superimposed image of the treated gels (**E**), but not the control gels (**D**), have undergone MitoSNO-mediated S-nitrosation. Spots that appear yellow in both gels when the Cy3 and Cy5 false colour images are overlaid are persistently occluded thiols that exist in equal proportion in all conditions. Pr-S-S, intramolecular protein disulfides; Pr-S-SG, protein mixed disulfides with glutathione; Pr-SOH, protein sulfenic acids.

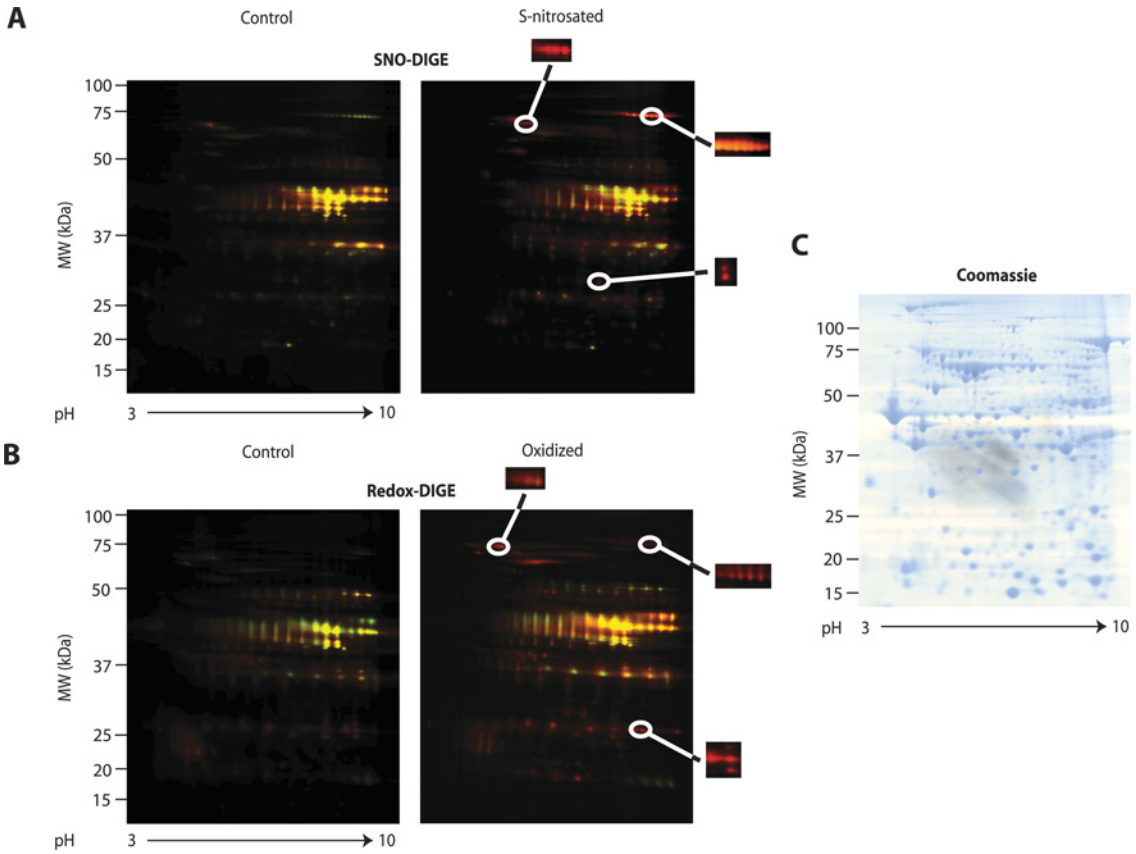

Figure 3 Effects of MitoSNO on mitochondrial protein thiols determined by SNO-DIGE and Redox-DIGE

Mitochondria were untreated or incubated with MitoSNO, and labelled with Cy5 maleimide (red) following either S-nitrosothiol specific reduction (**A**, SNO-DIGE) or non-specific reduction (**B**, Redox-DIGE). Cy5-labelled samples were combined separately with a Cy3-labelled sample (green) pooled from all replicate experiments and resolved on the same 2D gel. The superimposed fluorescent scans of representative gels from each triplicate experimental condition are shown. Gels used for identification of proteins of interest by MS were subsequently stained with Coomassie Blue (**C**).

glutathionylation or sulfenic acid modifications [2,25–27]. To distinguish those proteins that are persistently S-nitrosated from those that go on to form other thiol modifications, or which are directly oxidized in the S-nitrosating conditions, we conducted a Redox-DIGE analysis in parallel on these samples. Redox-DIGE identifies proteins that undergo all reversible thiol modifications, including S-nitrosation [9], therefore all spots that are positive for modification by Redox-DIGE should include those identified by SNO-DIGE and perhaps additional candidates. The parallel analysis of samples by Redox-DIGE revealed a number of thiol modifications induced by MitoSNO (Figure 3B).

Comparison of S-nitrosated mitochondrial protein thiols by SNO-DIGE and oxidized protein thiols by Redox-DIGE

Both SNO-DIGE and Redox-DIGE analyses showed that a number of proteins were S-nitrosated and/or had thiols oxidized on exposure to MitoSNO when compared with control incubations (Figures 3A and 3B). To determine whether an observed difference in fluorescence between the control and treated groups was due to a statistically significant alteration to the protein thiols of interest, we employed a threshold requiring a fluorescence ratio difference >2 ($P < 0.05$). According to these criteria, 18 spots corresponding to distinct proteins were found to show significant differences according to SNO-DIGE analysis, whereas 23 such spots were found according to Redox-DIGE analysis. As expected, there was considerable overlap between the identities of the proteins corresponding to these spots. Importantly, all but three proteins showing changes with SNO-DIGE also did so with Redox-DIGE. No false positives were observed (in which fluorescent ratios were significantly higher in control gels versus S-nitrosated samples), suggesting that the selection criteria used were sufficiently stringent.

Identification of S-nitrosated and oxidatively modified mitochondrial thiol proteins

The DIGE analyses enabled us to locate mitochondrial protein spots on a 2D gel that underwent a statistically significant change in Cy5 fluorescence intensity following treatment with MitoSNO and PrSNO specific reduction of thiols (SNO-DIGE), or reduction of all reversible thiol modifications (Redox-DIGE). To identify these proteins we excised gel spots from Coomassie Blue-stained gels (Figure 3C) matched to the Cy fluorescent images, and identified the proteins by MALDI–TOF-TOF MS. A Coomassie Blue-stained gel indicating the locations of the selected protein spots is shown in Supplementary Figure S2 (at http://www.BiochemJ.org/bj/430/bj4300049add.htm), and all proteins that could be unambiguously identified by these means are listed in Table 1. Of the spots corresponding to single proteins classified as significant from the analyses, 13 of 18 from the SNO-DIGE analysis and 16 of 23 from the Redox-DIGE analysis were identified. Table 1(A) lists the 13 proteins identified as being S-nitrosated from the SNO-DIGE analysis, whereas Table 1(B)

Table 1 Mitochondrial proteins containing thiols sensitive to modification by MitoSNO as identified by SNO-DIGE or Redox-DIGE

Thiol proteins sensitive to S-nitrosation (A) and oxidative modification (B) due to MitoSNO treatment are listed. The predicted molecular mass (MM) and isoelectric points (pI, in parentheses) of mature proteins are shown and are found in all cases to match closely to those observed on the gels. MASCOT PMF scores>59 (*Rattus* entries) for the peptide ion masses searched are significant ($P < 0.05$). For the tandem MS fragment ion masses, the number of significant ($P < 0.05$) MASCOT peptides are listed. Mean fluorescence ratios between the MitoSNO-treated and control values are listed for proteins showing a significant difference in either SNO-DIGE or Redox-DIGE analyses (difference > 2), as well as the associated *P*-values (one-way ANOVA; $^{**}P < 0.01$; $^{*}P < 0.05$). The number of cysteine residues contained in each mature protein of interest is provided, as well as a summary of the novelty of candidate identification. IPC, ischemic preconditioning.

Candidate			MS data			DIGE analysis summary			Literature Summary
NCBInr 'gi' accession	Protein name	MM (pI)	% Sequence coverage	MASCOT PMF score	Number of peptide sequences (MS/MS)	SNO analysis fluorescence ratio	Redox analysis fluorescence ratio	Cysteine residues	Identified as a target for S-nitrosation or thiol oxidation
(A)									
	TCA cycle								
40538860	Mitochondrial aconitase	82462 (7.15)	37	463	5	3.18**	2.58**	12	[7] (IPC/GSNO)
62945278	α-KGDH	111686 (6.00)	12	173	3	6.06**	2.31**	19	[7] (IPC)
18426858	Succinate dehydrogenase, subunit A flavoprotein	68004 (6.17)	29	478	6	2.30*	3.00	18	The present study
	Fatty acid catabolism								
6978435	Very long chain acyl-CoA dehydrogenase	66382 (8.10)	17	110	2	2.62**	5.15**	6	The present study
11968090	Short chain acyl-CoA dehydrogenase	42187 (6.38)	15	73	1	2.47*	2.00*	5	The present study
2392291	Enoyl-CoA hydratase	28287 (6.41)	36	160	2	2.29**	1.95	5	The present study
52138635	Electron-transferring flavoprotein dehydrogenase	64483 (6.47)	21	261	3	3.40**	2.68**	11	The present study
1850592	Carnitine palmitoyl transferase 2	71262 (6.43)	49	520	4	2.81**	2.74**	9	The present study
	Other metabolic enzymes								
51948476	Complex III, core protein 1	49380 (5.22)	10	165	2	2.17**	2.13	9	The present study
14192933	ALDH2 (mitochondrial)	54368 (5.69)	9	180	3	2.20**	3.98	9	[20] (GSNO/SNAP)
	Other								
62079055	Isocitrate dehydrogenase (NADP+)	46640 (8.49)	20	94	2	2.06**	2.66**	11	The present study
25742763	78 kDa Glucose regulated protein	72302 (5.07)	19	415	4	7.00**	Not focused	3	The present study
3915779	Myosin heavy chain 6	223488 (5.68)	15	432	6	2.95*	2.24**	14	[7] (IPC)
(B)									
57527204	Electron-transferring flavoprotein α polypeptide	34929 (8.62)	31	437	4	1.26	4.04*	6	[7] (GSNO)
6978431	Long chain acyl-CoA dehydrogenase	44672 (6.26)	33	272	4	0.88	2.00**	6	The present study
20304123	3-Mercaptopyruvate sulfurtransferase	32809 (5.88)	28	277	4	1.25	2.83**	5	The present study
149036390	Mitofilin	83484 (6.18)	27	319	3	0.86	7.84*	7	The present study

lists the four additional proteins found to be oxidatively modified by the Redox-DIGE analysis following MitoSNO-treatment, but which were not detected by SNO-DIGE. One observed discrepancy between the analyses is due to the 78 kDa glucose-regulated protein, which was detected by the SNO-DIGE analysis, but was poorly focused on the 2D gels during the Redox-DIGE analysis. Consequently, a reliable fluorescence ratio was not obtained (Table 1). Additionally, a small number of candidates from the SNO-DIGE analysis fell just below the threshold of significance (fluorescence ratio >2, $P < .05$) in the Redox-DIGE analysis (Table 1). The mean fluorescence ratio between MitoSNO treated and control spots are included from both analyses, the number of cysteine residues contained in each identified protein, and a summary of the MS data used to identify the protein are also provided in Table 1. Additionally, we indicated whether the candidate proteins have previously been reliably reported as targets for S-nitrosation. The MS data used to identify the proteins are more fully described in Supplementary Table S2 (at http://www.BiochemJ.org/bj/430/bj4300049add.htm). As shown in Table 1(A), the fluorescence ratios obtained for the S-nitrosated proteins by the SNO-DIGE and Redox-DIGE analyses for most proteins are very similar. This suggests that for these proteins, the change in thiol redox state indicated by Redox-DIGE was due largely to S-nitrosation and that other thiol redox modifications did not occur to a significant extent. One exception is the very long chain acyl-CoA dehydrogenase, which had a nearly 2-fold higher fluorescence ratio by Redox-DIGE analysis over SNO-DIGE, suggesting that a significant proportion of this enzyme was both S-nitrosated and oxidatively modified. Interestingly, although nearly all of the S-nitrosated proteins identified are involved in mitochondrial metabolism, Redox-DIGE analysis identified mitofilin, a mitochondrial membrane protein that is thought to be involved in modulating cristae morphology [28], as a target for thiol oxidation due to MitoSNO action.

It is noteworthy that nearly all of the mitochondrial proteins identified by SNO-DIGE and by Redox-DIGE are found in the mitochondrial matrix compartment, with two exceptions. The 78 kDa glucose-regulated protein is generally regarded as an endoplasmic reticulum protein, however, it has been reported to be present in mitochondrial matrix [29]. Also, myosin heavy chain VI has not been reported as being associated with mitochondria and is involved with intracellular vesicle trafficking [30].

S-nitrosation of metabolic enzymes by MitoSNO results in reversible inhibition

SNO-DIGE analysis identified a small number of heart mitochondrial proteins that were persistently S-nitrosated by MitoSNO. Surprisingly, the majority of novel targets identified are enzymes central to mitochondrial metabolism, so these proteins are all candidates for the biological consequences of mitochondrial S-nitrosation through regulation of mitochondrial function. However, for this to be the case S-nitrosation must affect enzyme activity. To determine if this occurred, we selected three candidate enzymes from the proteins identified as targets of S-nitrosation: mitochondrial aconitase, α-KGDH

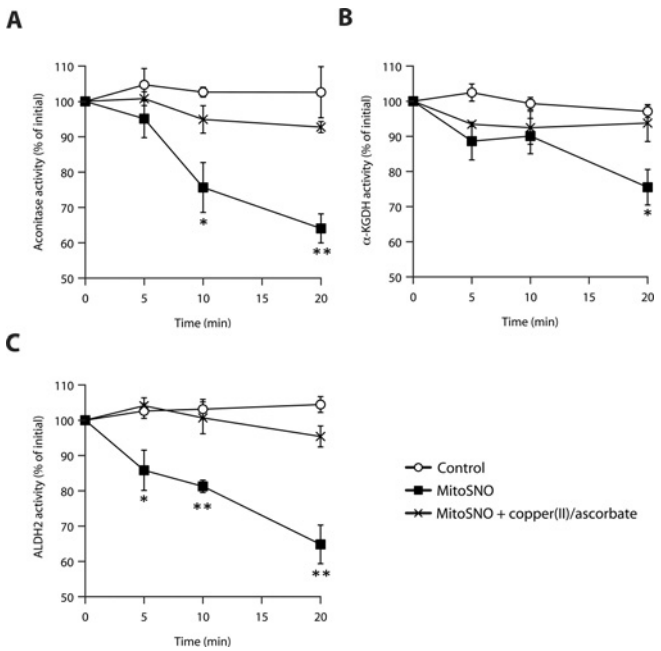

Figure 4 Reversible inhibition of enzyme activity due to S-nitrosation by MitoSNO

Metabolic enzymes found to be S-nitrosated from the SNO-DIGE analysis were measured for changes in activity due to MitoSNO action. (**A**) Mitochondrial aconitase activity was found to decrease, beginning 5 min following MitoSNO treatment and showing significant inhibition beyond 10 min when compared with the vehicle control. Addition of copper(II) and ascorbate to selectively reduce PrSNOs following treatment with MitoSNO completely reversed the inhibitory effect. (**B**) α-KGDH activity was also inhibited by MitoSNO action, causing significant inhibition 20 min following MitoSNO addition. The inhibitory effect of MitoSNO was reversed by copper(II) and ascorbate. (**C**) MitoSNO significantly inhibited mitochondrial ALDH2 5 min following its addition and onwards, and the inhibitory effect was completely reversed by copper(II) and ascorbate. Error bars show means $\pm$ S.E.M.; $^*P < 0.05$; $^{**}P < 0.01$ by Student's *t* test.

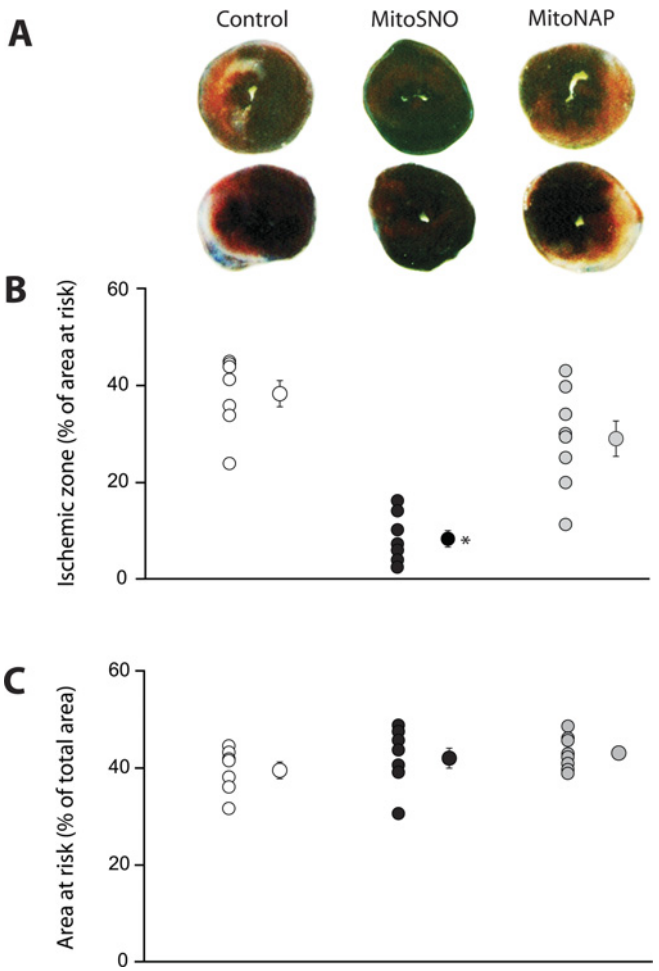

Figure 5 MitoSNO is protective against cardiac I/R injury *in vivo*

Cardiac I/R injury was established in a mouse *in vivo* model by LAD occlusion for 30 min, followed by reperfusion and 24 h recovery, at which point the area of infarcted heart tissue was determined. MitoSNO or MitoNAP (100 ng/kg), or vehicle carrier, was injected directly into the left ventricle after 25 min ischaemia, 5 min prior to reperfusion. (**A**) Two representative formalin-fixed heart cross-sectional images at the center of ventricles for each condition. Dark blue, non-risk zone; pale white, necrotic infarcted tissue; deep red, live tissue. (**B**) Quantification of the infarct size as a percentage of the AR. Data from individual experiments are shown on the left and the means $\pm$ S.E.M. is shown on the right. ○, vehicle carrier; ●, MitoSNO; ◍, MitoNAP. (**C**) Quantification of the proportion of entire heart tissue identified as AR in the same groups. $n = 7$–8 per group; $^*P < 0.05$ by between groups ANOVA.

and mitochondrial ALDH2. Both aconitase and α-KGDH are citric acid cycle enzymes and central to mitochondrial energetics, whereas ALDH2 is a key enzyme in the NAD^+-dependent detoxification of aldehydes [31].

The activities of all three enzymes were significantly and progressively inhibited by MitoSNO (Figure 4), whereas the control compound MitoNAP, which lacks an S-nitrosating moiety but is identical to MitoSNO in every other respect, had no effect (see Supplementary Figure S3 at http://www.BiochemJ.org/bj/430/bj4300049add.htm). Subsequent removal of NO from the PrSNO by incubation of S-nitrosated mitochondrial extracts with DTT restored activity for all three enzymes (Supplementary Figure S3). However, although DTT will reverse S-nitrosation, it is not selective and will reverse many other thiol modifications. Therefore we treated S-nitrosated mitochondrial samples with copper(II) and ascorbate to selectively degrade *S*-nitrosothiols and found that this treatment completely restored the activity of all three enzymes (Figure 4). Control experiments showed that inhibition of the enzymes by the thiol oxidant diamide was not reversed by copper(II) and ascorbate treatment (results not shown), corroborating our previous results showing that this reduction is highly selective for PrSNOs [6]. These findings not only demonstrate the mechanistic consequences of S-nitrosation for these candidate proteins, but establish the full reversibility of the modification using the same selective reduction by copper(II) and ascorbate employed for the SNO-DIGE method.

MitoSNO protects against cardiac I/R injury *in vivo*

Since mitochondrial S-nitrosation correlates with protection in I/R injury, we examined whether MitoSNO would be protective. To do so, we made use of the well-established murine model of *in vivo* I/R injury by subjecting mice to occlusion of the LAD for 30 min followed by reperfusion and recovery over 24 h [21]. Following the recovery period, analysis of the heart showed significant damage, as indicated by the area of infarcted tissue (Figure 5A, white tissue), and by comparison of the infarcted zone to the AR (Figures 5B and 5C). In contrast, injection of MitoSNO into the left ventricle 5 min prior to reperfusion significantly decreased heart damage (Figures 5A and 5B). Control injections with MitoNAP, the MitoSNO precursor that lacks the *S*-nitrosothiol, were not protective (Figure 5).

DISCUSSION

Protein S-nitrosation has emerged as a significant component of NO action within mitochondria [1,2,4], although the breadth and consequences of mitochondrial protein S-nitrosation are not yet fully understood. To help address this, we set out to identify mitochondrial thiol proteins that were susceptible to S-nitrosation. To do so we used MitoSNO, a mitochondria-targeted *S*-nitrosothiol [6], because the cohort of mitochondrial proteins that are S-nitrosated by MitoSNO is likely to be similar to those proteins that are S-nitrosated under physiological conditions [6].

To identify these S-nitrosated mitochondrial thiol proteins, we developed a sensitive and selective proteomic technique, SNO-DIGE (Figure 2). By making use of the highly specific reduction of protein *S*-nitrosothiols by copper(II) and ascorbate, DIGE to resolve the mitochondrial proteome, and an experimental design incorporating sample pooling based on BVA, we were able to obtain highly reproducible results and avoid variability associated with comparing gel pairs and replicates. A central advantage of the DIGE approach is its reliance on sensitive fluorescence detection, which allows for the identification of low-abundance proteins [9,32]. The SNO-DIGE method further extends this sensitivity to facilitate the robust detection of the low-abundance targets for *S*-nitrosation. Previously, studies using DIGE methods to identify PrSNOs have relied on the comparison of protein from different biological sources within one gel [7,33], so that control protein was derived from a different specimen from treated protein. This design does not account for the effect of biological variability due to differences in individual protein abundance between replicates as opposed to differences due to S-nitrosation, thereby significantly increasing signal noise, and the chances of false negative and false positive results [13,34]. In the present study we compared changes in S-nitrosation from the same biological source, effectively controlling for biological variability. In addition, we made use of a pooled standard in each gel comprising equal amounts of protein from all biological replicates. This approach significantly reduces both biological and technical variability, increasing the statistical power of the analysis [13,34]. It also controls for dye-specific effects and overcomes the difficulty of matching gel pairs to obtain reliable and semi-quantitative results [8,35,36]. Finally, the SNO-DIGE method is the first to make use of the copper(I)-dependent PrSNO reduction in a proteomic screen [11], which has been shown by our group and others to be a highly specific means of reducing PrSNOs and leaving other reversible thiol modifications unaffected (Supplementary Figure S2) [6,11]. Previous studies have either relied on ascorbate reduction in the presence of copper chelators [7] or on higher concentrations (5–10 mM) of ascorbate [33,37], which have been shown to be insufficient and non-specific methods for PrSNO reduction respectively [11,38–41]. In summary, the SNO-DIGE method provides a significant improvement in specificity, sensitivity and reproducibility for proteomic screens of PrSNOs, which is essential for the robust identification of such a scarce modification, and can be applied to the identification of S-nitrosated proteins in many other systems.

A potential limitation of the SNO-DIGE approach is the requirement for 2D electrophoresis, which under-represents hydrophobic membrane proteins [9]. It is also possible that the S-nitrosation of proteins containing a number of occluded thiols, such as iron-sulfur proteins, may be difficult to detect by this procedure. This arises from the fact that initially unreactive thiols may become exposed and then show strong labelling by both the Cy3 and Cy5 dye, resulting in spots with equally intense fluorescence in both channels (appearing yellow) on the gels that may mask changes occurring on other thiols on the same or on a co-localized protein. These are likely to be the reasons why complex I, which is known to be S-nitrosated by MitoSNO [6], was not detected by this screen as its subunits are hydrophobic or contain many iron-sulfur centres. However, the principles underlying the SNO-DIGE methodology are easily adaptable to other gel systems and should enable these restrictions to be overcome ([6] and E. Chouchani and M. P. Murphy, unpublished work). Finally, although SNO-DIGE allows for robust protein identification, reliable assessment of the modified cysteine residue(s) is not possible. Knowledge of the cysteine residue modified in candidate proteins and the extent of their S-nitrosation are vital for understanding the physiological and pathological consequences of mitochondrial S-nitrosation. To do this, further studies are underway using orthogonal approaches to determine the residues affected in the candidate proteins identified by SNO-DIGE and to quantify their extent of S-nitrosation.

Application of the SNO-DIGE method to heart mitochondria allowed us to identify a number of novel proteins that contained thiols sensitive to persistent S-nitrosation, as well as to corroborate targets that have been identified previously (Table 1). A parallel Redox-DIGE analysis determined that the majority of thiol modifications due to MitoSNO action were indeed persistent S-nitrosation. Only three proteins modified in the SNO-DIGE analysis were not also found in the Redox-DIGE analysis. Those not found were either just below the threshold of significance or were poorly focused in the Redox-DIGE gels, resulting in the inability to match spots across gels and obtain statistical significance. These findings also indicated that there was a small pool of thiol proteins that underwent thiol oxidation but were not S-nitrosated under these conditions. This is likely to occur due to transient S-nitrosation of mitochondrial proteins followed by subsequent relaxation of the *S*-nitrosothiol to other thiol redox modifications [2]. Alternatively, these proteins may become oxidized as a consequence of the effect of S-nitrosation of other mitochondrial proteins. These complementary findings from the two DIGE analyses exemplify the reproducibility of the two techniques, whereas the number of newly identified candidate proteins for S-nitrosation demonstrates the significantly improved specificity and sensitivity of the SNO-DIGE methodology.

The cohort of proteins modified by MitoSNO contrasts with those affected by incubation of mitochondria with the non-targeted S-nitrosating agent SNAP [9], which were predominantly outer membrane proteins or contaminating cytosolic proteins. This discrepancy is probably due to the extensive and selective uptake of MitoSNO into mitochondria driven by membrane potential and leading to the selective S-nitrosation of matrix proteins [6]. Interestingly, the majority of proteins identified were metabolic enzymes responsible for both carbohydrate and fatty acid oxidation. Five enzymes involved in the oxidation of fatty acids were identified as targets for S-nitrosation. These include the very-long-chain acyl-CoA dehydrogenase, short-chain acyl-CoA dehydrogenase and enoyl-CoA hydratase, which catalyse the initial oxidation step and subsequent hydration of unsaturated carbons in the β-oxidation pathway of very-long-chain and short-chain fatty acids [42]. Also identified were carnitine palmitoyl transferase 2 and the electron-transferring flavoprotein dehydrogenase, which are responsible for the initiation of β-oxidation and final supply of electrons from fatty acid catabolism to the mitochondrial Q-pool [43] respectively. Interestingly, three citric acid cycle enzymes were also identified by SNO-DIGE: aconitase, which catalyses the initial isomerization of citrate; α-KGDH, which catalyses the NADH-coupled oxidation of α-ketoglutarate; and succinate dehydrogenase, which oxidizes succinate to reduce the Q-pool. These findings indicate that the

S-nitrosation of mitochondrial protein thiols targets a number of enzymes central to mitochondrial metabolism, specifically those supplying electrons to the respiratory chain from the breakdown of both carbohydrates and fatty acids.

In addition to those proteins involved in metabolism, mitofilin was identified as containing redox-sensitive thiols. Although the function of mitofilin has not been fully elucidated, it has been suggested that it modulates mitochondrial cristae organization [28], and participates in protein import into the matrix [44]. Although several studies highlight the detrimental effects of mitofilin depletion, this is the first indication that it may be responsive to redox regulation and may suggest a role for mitofilin in the response of mitochondrial morphology to oxidative stress and redox signalling.

To determine the functional consequences of S-nitrosation, its impact was assessed on the activity of three of the enzymes indentified in the SNO-DIGE screen: mitochondrial aconitase, α-KGDH and ALDH2. S-nitrosation correlated with inhibition of all three enzymes, and these decreases in activity were reversed by reducing *S*-nitrosothiols with DTT (Supplementary Figure S3) and by treatment with copper(II) and ascorbate (Figure 4), which is selective for the reduction of *S*-nitrosothiols. These results were significant as they provided an orthogonal validation for the proteomic screen and showed that the proteins identified by SNO-DIGE were indeed susceptible to S-nitrosation. In addition, these findings indicated that the S-nitrosation by MitoSNO had functional consequences for these enzymes, that this decrease in activity was due to S-nitrosation, and that inhibition was readily reversible by specific reduction of the *S*-nitrosothiol. This is consistent with the reversible S-nitrosation of mitochondrial proteins being involved in the regulation of mitochondrial function. The reversal of inhibition by copper(II) and ascorbate also indicates that the treatment used for PrSNO reduction in SNO-DIGE is mild and has minimal damaging side effects on proteins.

Exploring the functional effects of S-nitrosation of central mitochondrial enzymes provided insights regarding their interaction with NO. Mitochondrial aconitase is known to be inactivated by superoxide and peroxynitrite, whereas inhibition due to NO is thought to occur only at high non-physiological concentrations [18]. In contrast, here we have demonstrated that aconitase can be readily S-nitrosated by low concentrations of MitoSNO, resulting in moderate inhibition of enzyme activity, which is reversible upon reduction of the *S*-nitrosothiol (Figure 4A). This is likely to be due to the reversible *S*-nitrosation of a cysteine residue on aconitase; however, we cannot exclude the possibility of a contribution from a putative reversible [4Fe-4S]-NO adduct of the active site iron centre [45]. Interestingly, the NO-donor GSNO (*S*-nitrosoglutathione) has been shown to irreversibly inactivate aconitase, suggesting either discrepant mechanisms of inactivation exist or perhaps that irreversible inactivation occurs following only prolonged exposure to very high concentrations of NO donors [45]. α-KGDH has been suggested as a target of S-nitrosation previously, but not unequivocally identified as such [7]. Its activity has been shown to increase following addition of very high concentrations of GSNO, but this change was not tested for reversibility [7]. Our SNO-DIGE analysis corroborated that α-KGDH can be S-nitrosated, but under our S-nitrosating conditions there was a moderate decrease in activity that was reversed by reduction of the *S*-nitrosothiol (Figure 4B). The S-nitrosation of ALDH2 by high (0.5 and 1.0 mM) concentrations of GSNO and SNAP inhibits its activity in rat hepatoma cells [20]. We demonstrated a similar moderate inhibition by MitoSNO-induced S-nitrosation that was completely reversible (Figure 4C).

The findings that S-nitrosation inhibits a number of mitochondrial metabolic enzymes extends previous work showing that S-nitrosation of complex I decreases its activity [2,6]. The inhibition of complex I has been suggested to be protective during I/R injury by preventing mitochondrial ROS production and calcium overloading [2,6,46,47]. It may be that the mild, reversible inhibition by S-nitrosation of citric acid cycle and β-oxidation enzymes also contributes to this process by preventing the build up of NADH and a reduced Q-pool during I/R which may produce a burst of damaging free radicals during reperfusion [48]. Additionally, it has been suggested that the S-nitrosation of thiol proteins may also act to prevent their irreversible inactivation by oxidative damage [49]. Consistent with these findings, in a preliminary experiment we found that administration of just 100 ng/kg of MitoSNO was protective in an *in vivo* model of cardiac I/R injury. Thus MitoSNO is significantly more potent that other cardioprotective NO donors when administered just prior to the reperfusion phase of I/R injury (Figure 5) [7,21,50]. This is consistent with rapid uptake of MitoSNO into mitochondria and S-nitrosation of mitochondrial proteins [6]. Thus MitoSNO may protect during I/R injury partly by inhibiting central metabolic enzymes, decreasing mitochondrial oxidative damage through limiting substrate supply and by protecting protein thiols from irreversible oxidation. However, future work will be required to establish the role of mitochondrial protein *S*-nitrosation *in vivo* and its potential contribution to the protective effect observed in I/R injury.

In summary, we have developed a proteomic method, SNO-DIGE, for the highly selective identification of low-abundance S-nitrosated protein thiols. We have used this method to identify a number of novel mitochondrial targets of S-nitrosation. The majority of these targets were enzymes responsible for carbohydrate and fatty acid catabolism, and we demonstrated that for three of these targets S-nitrosation reversibly inhibited enzymatic activity. These findings are consistent with the S-nitrosation of mitochondrial proteins regulating mitochondrial energetics and function, providing insight into the physiological and pathological roles of NO.

AUTHOR CONTRIBUTION

Edward Chouchani designed and carried out the mitochondrial and DIGE experiments and co-wrote the paper. Sergiy Nadtochiy and Paul Brookes carried out the I/R experiments. Thomas Hurd and Kathryn Lilley assisted in the interpretation of the DIGE data. Ian Fearnley supervised protein identification by MS. Robin Smith helped develop the rationale for the project and supervised the synthesis of MitoSNO. Michael Murphy oversaw the project and co-wrote the paper.

FUNDING

This work was supported by the Medical Research Council, by a post-graduate scholarship from the Gates Cambridge Trust (to E.T.C) and by the National Institutes of Health [grant number HL-071158].

ACKNOWLEDGEMENTS

We thank Renata Feret and Dr Kamburapola Jayawardena for technical assistance with the DIGE and MS analysis, and Dr Andrew James for helpful discussions.

REFERENCES

1 Moncada, S. and Erusalimsky, J. D. (2002) Does nitric oxide modulate mitochondrial energy generation and apoptosis? Nat. Rev. Mol. Cell Biol. **3**, 214–220

2 Dahm, C. C., Moore, K. and Murphy, M. P. (2006) Persistent S-nitrosation of complex I and other mitochondrial membrane proteins by S-nitrosothiols but not nitric oxide or peroxynitrite: implications for the interaction of nitric oxide with mitochondria. J. Biol. Chem. **281**, 10056–10065

3 Gao, S., Chen, J., Brodsky, S. V., Huang, H., Adler, S., Lee, J. H., Dhadwal, N., Cohen-Gould, L., Gross, S. S. and Goligorsky, M. S. (2004) Docking of endothelial nitric oxide synthase (eNOS) to the mitochondrial outer membrane: a pentabasic amino acid sequence in the autoinhibitory domain of eNOS targets a proteinase K-cleavable peptide on the cytoplasmic face of mitochondria. J. Biol. Chem. **279**, 15968–15974

4 Hogg, N. (2002) The biochemistry and physiology of S-nitrosothiols. Annu. Rev. Pharmacol. Toxicol. **42**, 585–600

5 van der Vliet, A., Hoen, P. A., Wong, P. S., Bast, A. and Cross, C. E. (1998) Formation of S-nitrosothiols via direct nucleophilic nitrosation of thiols by peroxynitrite with elimination of hydrogen peroxide. J. Biol. Chem. **273**, 30255–30262

6 Prime, T. A., Blaikie, F. H., Evans, C., Nadtochiy, S. M., James, A. M., Dahm, C. C., Vitturi, D. A., Patel, R. P., Hiley, C. R., Abakumova, I. et al. (2009) A mitochondria-targeted S-nitrosothiol modulates respiration, nitrosates thiols, and protects against ischemia-reperfusion injury. Proc. Natl. Acad. Sci. U.S.A. **106**, 10764–10769

7 Sun, J., Morgan, M., Shen, R. F., Steenbergen, C. and Murphy, E. (2007) Preconditioning results in S-nitrosylation of proteins involved in regulation of mitochondrial energetics and calcium transport. Circ. Res. **101**, 1155–1163

8 Unlu, M., Morgan, M. E. and Minden, J. S. (1997) Difference gel electrophoresis: a single gel method for detecting changes in protein extracts. Electrophoresis **18**, 2071–2077

9 Hurd, T. R., Prime, T. A., Harbour, M. E., Lilley, K. S. and Murphy, M. P. (2007) Detection of reactive oxygen species-sensitive thiol proteins by redox difference gel electrophoresis: implications for mitochondrial redox signaling. J. Biol. Chem. **282**, 22040–22051

10 Hurd, T. R., James, A. M., Lilley, K. S. and Murphy, M. P. (2009) Chapter 19 Measuring redox changes to mitochondrial protein thiols with redox difference gel electrophoresis (redox-DIGE). Methods Enzymol. **456**, 343–361

11 Wang, X., Kettenhofen, N. J., Shiva, S., Hogg, N. and Gladwin, M. T. (2008) Copper dependence of the biotin switch assay: modified assay for measuring cellular and blood nitrosated proteins. Free Radical Biol. Med. **44**, 1362–1372

12 Marouga, R., David, S. and Hawkins, E. (2005) The development of the DIGE system: 2D fluorescence difference gel analysis technology. Anal. Bioanal. Chem. **382**, 669–678

13 Karp, N. A. and Lilley, K. S. (2009) Investigating sample pooling strategies for DIGE experiments to address biological variability. Proteomics **9**, 388–397

14 Chappell, J. B. and Hansford, R. G. (1972) Preparation of mitochondria from animal tissues and yeasts. In Subcellular Components: Preparation and Fractionation (Birnie, G.D., ed.). pp. 77–91, Butterworths, London

15 Gornall, A. G., Bardawill, C. J. and David, M. M. (1949) Determination of serum protein by means of the biuret reaction. J. Biol. Chem. **177**, 751–766

16 Wilm, M., Shevchenko, A., Houthaeve, T., Breit, S., Schweigerer, L., Fotsis, T. and Mann, M. (1996) Femtomole sequencing of proteins from polyacrylamide gels by nano-electrospray mass spectrometry. Nature **379**, 466–469

17 Perkins, D. N., Pappin, D. J., Creasy, D. M. and Cottrell, J. S. (1999) Probability-based protein identification by searching sequence databases using mass spectrometry data. Electrophoresis **20**, 3551–3567

18 Gardner, P. R. (2002) Aconitase: sensitive target and measure of superoxide. Methods Enzymol. **349**, 9–23

19 Lai, J. C. and Cooper, A. J. (1986) Brain α-ketoglutarate dehydrogenase complex: kinetic properties, regional distribution, and effects of inhibitors. J. Neurochem. **47**, 1376–1386

20 Moon, K. H., Kim, B. J. and Song, B. J. (2005) Inhibition of mitochondrial aldehyde dehydrogenase by nitric oxide-mediated S-nitrosylation. FEBS Lett. **579**, 6115–6120

21 Nadtochiy, S. M., Burwell, L. S., Ingraham, C. A., Spencer, C. M., Friedman, A. E., Pinkert, C. A. and Brookes, P. S. (2009) *In vivo* cardioprotection by S-nitroso-2-mercaptopropionyl glycine. J. Mol. Cell. Cardiol. **46**, 960–968

22 Shaw, J., Rowlinson, R., Nickson, J., Stone, T., Sweet, A., Williams, K. and Tonge, R. (2003) Evaluation of saturation labelling two-dimensional difference gel electrophoresis fluorescent dyes. Proteomics **3**, 1181–1195

23 Lilley, K. S. and Dupree, P. (2006) Methods of quantitative proteomics and their application to plant organelle characterization. J. Exp. Bot. **57**, 1493–1499

24 Kreil, D. P., Karp, N. A. and Lilley, K. S. (2004) DNA microarray normalization methods can remove bias from differential protein expression analysis of 2D difference gel electrophoresis results. Bioinformatics **20**, 2026–2034

25 Becker, K., Savvides, S. N., Keese, M., Schirmer, R. H. and Karplus, P. A. (1998) Enzyme inactivation through sulfhydryl oxidation by physiologic NO-carriers. Nat. Struct. Biol. **5**, 267–271

26 Shiva, S., Crawford, J. H., Ramachandran, A., Ceaser, E. K., Hillson, T., Brookes, P. S., Patel, R. P. and Darley-Usmar, V. M. (2004) Mechanisms of the interaction of nitroxyl with mitochondria. Biochem. J. **379**, 359–366

27 Chen, Y. R., Chen, C. L., Pfeiffer, D. R. and Zweier, J. L. (2007) Mitochondrial complex II in the post-ischemic heart: oxidative injury and the role of protein S-glutathionylation. J. Biol. Chem. **282**, 32640–32654

28 John, G. B., Shang, Y., Li, L., Renken, C., Mannella, C. A., Selker, J. M., Rangell, L., Bennett, M. J. and Zha, J. (2005) The mitochondrial inner membrane protein mitofilin controls cristae morphology. Mol. Biol. Cell **16**, 1543–1554

29 Sun, F. C., Wei, S., Li, C. W., Chang, Y. S., Chao, C. C. and Lai, Y. K. (2006) Localization of GRP78 to mitochondria under the unfolded protein response. Biochem. J. **396**, 31–39

30 Buss, F., Arden, S. D., Lindsay, M., Luzio, J. P. and Kendrick-Jones, J. (2001) Myosin VI isoform localized to clathrin-coated vesicles with a role in clathrin-mediated endocytosis. EMBO J. **20**, 3676–3684

31 Svanas, G. W. and Weiner, H. (1985) Aldehyde dehydrogenase activity as the rate-limiting factor for acetaldehyde metabolism in rat liver. Arch. Biochem. Biophys. **236**, 36–46

32 Fu, C., Hu, J., Liu, T., Ago, T., Sadoshima, J. and Li, H. (2008) Quantitative analysis of redox-sensitive proteome with DIGE and ICAT. J. Proteome Res. **7**, 3789–3802

33 Santhanam, L., Gucek, M., Brown, T. R., Mansharamani, M., Ryoo, S., Lemmon, C. A., Romer, L., Shoukas, A. A., Berkowitz, D. E. and Cole, R. N. (2008) Selective fluorescent labeling of S-nitrosothiols (S-FLOS): a novel method for studying S-nitrosation. Nitric Oxide **19**, 295–302

34 Weinkauf, M., Hiddemann, W. and Dreyling, M. (2006) Sample pooling in 2-D gel electrophoresis: a new approach to reduce nonspecific expression background. Electrophoresis **27**, 4555–4558

35 Karp, N. A., Kreil, D. P. and Lilley, K. S. (2004) Determining a significant change in protein expression with DeCyder during a pair-wise comparison using two-dimensional difference gel electrophoresis. Proteomics **4**, 1421–1432

36 Karp, N. A. and Lilley, K. S. (2005) Maximising sensitivity for detecting changes in protein expression: experimental design using minimal CyDyes. Proteomics **5**, 3105–3115

37 Moon, K. H., Hood, B. L., Kim, B. J., Hardwick, J. P., Conrads, T. P., Veenstra, T. D. and Song, B. J. (2006) Inactivation of oxidized and S-nitrosylated mitochondrial proteins in alcoholic fatty liver of rats. Hepatology **44**, 1218–1230

38 Smith, J. N. and Dasgupta, T. P. (2000) Kinetics and mechanism of the decomposition of S-nitrosoglutathione by L-ascorbic acid and copper ions in aqueous solution to produce nitric oxide. Nitric Oxide **4**, 57–66

39 Kashiba-Iwatsuki, M., Yamaguchi, M. and Inoue, M. (1996) Role of ascorbic acid in the metabolism of S-nitroso-glutathione. FEBS Lett. **389**, 149–152

40 Huang, B. and Chen, C. (2006) An ascorbate-dependent artifact that interferes with the interpretation of the biotin switch assay. Free Radical Biol. Med. **41**, 562–567

41 Landino, L. M., Koumas, M. T., Mason, C. E. and Alston, J. A. (2006) Ascorbic acid reduction of microtubule protein disulfides and its relevance to protein S-nitrosylation assays. Biochem. Biophys. Res. Commun. **340**, 347–352

42 Bartlett, K. and Eaton, S. (2004) Mitochondrial β-oxidation. Eur. J. Biochem. **271**, 462–469

43 Ramsay, R. R., Steenkamp, D. J. and Husain, M. (1987) Reactions of electron-transfer flavoprotein and electron-transfer flavoprotein: ubiquinone oxidoreductase. Biochem. J. **241**, 883–892

44 Rossi, M. N., Carbone, M., Mostocotto, C., Mancone, C., Tripodi, M., Maione, R. and Amati, P. (2009) Mitochondrial localization of PARP-1 requires interaction with mitofilin and is involved in the maintenance of mitochondrial DNA integrity. J. Biol. Chem. **284**, 31616–31624

45 Tortora, V., Quijano, C., Freeman, B., Radi, R. and Castro, L. (2007) Mitochondrial aconitase reaction with nitric oxide, S-nitrosoglutathione, and peroxynitrite: mechanisms and relative contributions to aconitase inactivation. Free Radical Biol. Med. **42**, 1075–1088

46 Nadtochiy, S. M., Burwell, L. S. and Brookes, P. S. (2007) Cardioprotection and mitochondrial S-nitrosation: effects of S-nitroso-2-mercaptopropionyl glycine (SNO-MPG) in cardiac ischemia-reperfusion injury. J. Mol. Cell. Cardiol. **42**, 812–825

47 Galkin, A., Abramov, A. Y., Frakich, N., Duchen, M. R. and Moncada, S. (2009) Lack of oxygen deactivates mitochondrial complex I: implications for ischemic injury? J. Biol. Chem. **284**, 36055–36061

48 Murphy, M. P. (2009) How mitochondria produce reactive oxygen species. Biochem. J. **417**, 1–13

49 Requejo, R., Hurd, T. R., Costa, N. J. and Murphy, M. P. (2010) Cysteine residues exposed on protein surfaces are the dominant intramitochondrial thiol and may protect against oxidative damage. FEBS J. **277**, 1465–1480

50 Bell, R. M., Maddock, H. L. and Yellon, D. M. (2003) The cardioprotective and mitochondrial depolarising properties of exogenous nitric oxide in mouse heart. Cardiovasc. Res. **57**, 405–415

Received 23 April 2010/9 June 2010; accepted 10 June 2010
Published as BJ Immediate Publication 10 June 2010, doi:10.1042/BJ20100633

Biochem. J. (2010) **430**, 49–59 (Printed in Great Britain) doi:10.1042/BJ20100633

online data

SUPPLEMENTARY ONLINE DATA

Identification of S-nitrosated mitochondrial proteins by *S*-nitrosothiol difference in gel electrophoresis (SNO-DIGE): implications for the regulation of mitochondrial function by reversible S-nitrosation

Edward T. CHOUCHANI*, Thomas R. HURD*, Sergiy M. NADTOCHIY†, Paul S. BROOKES†, Ian M. FEARNLEY*, Kathryn S. LILLEY‡, Robin A. J. SMITH§ and Michael P. MURPHY*[1]

*MRC Mitochondrial Biology Unit, Hills Road, Cambridge CB2 0XY, U.K., †Department of Anesthesiology, University of Rochester Medical Center, 601 Elmwood Avenue, Rochester, NY 14642, U.S.A., ‡Department of Biochemistry, Cambridge System Biology Centre, University of Cambridge, Cambridge CB2 1GA, U.K., and §Department of Chemistry, University of Otago, P.O. Box 56, Dunedin 9054, New Zealand

Table S1 Identity of thiol proteins containing occluded thiols determined by SNO-DIGE and Redox-DIGE

Protein spots were excised from 2D gels, digested with trypsin by the 'in-gel' cleavage method and analysed by MALDI–TOF-TOF MS. For peptide ion masses searched (MS data), MASCOT scores>59 (*Rattus* database) are significant ($P<0.05$). For the tandem MS fragment masses (supporting tandem MS data), the values required for significance ($P<0.05$) are reported in brackets after the MASCOT ion score. Amino acids are abbreviated using standard one character symbols. Residue numbers correspond to the complete protein sequences found in the NCBI database. The established nature of the occluded thiols for each candidate is included. MM, molecular mass.

Candidate			MS data				Supporting tandem MS data				
NCBInr 'gi' accession	Protein name	MM (pI)	% Sequence coverage	Peptide matches at 25 p.p.m./ supplied	MASCOT score	Observed	Mass (MH^+) calculated	Residues	Sequence	MASCOT score ($P < 0.05$)	Thiols
58865384	Complex I 49 kDa subunit	49243 (5.95)	29	18 of 45	355	934.5278	934.5363	172–179	VLFGEITR	50 (38)	Fe-S
						1047.6228	1047.6315	158–166	LLNIQPPPR	43 (38)	
						2228.1182	2228.0512	305–323	TQPYDVYDQVEFDVPIGSR	111 (38)	
51092268	Complex I 24 kDa subuit	23933 (5.07)	32	11 of 18	320	1244.6405	1244.6375	199–208	DIEEIIDELR	64 (29)	Fe-S
						1336.7994	1336.7953	75–87	AAAVLPVLDLAQR	63 (29)	
						2398.0083	2398.0112	42–61	DTPENNPDTPFDFTPENYER	126 (29)	
125313	Mitochondrial creatine kinase	43144 (7.78)	30	14 of 45	348	1390.6908	1390.7008	47–58	LFPPSADYPDLR	57 (38)	Exposed
						2109.0044	2109.0101	285–305	GTGGVDTAAVADVYDISNIDR	121 (38)	
						1673.8197	1673.8288	258–270	TFLIWINEEDHTR	59 (38)	
40786469	Dihydrolipoamide dehydrogenase	50089 (6.51)	20	12 of 41	217	1127.6536	1127.6578	133–143	ALTGGIAHLFK	42 (37)	Exposed
						1737.8724	1737.8825	90–104	ALLNNSHYYHLAHGK	73 (37)	
						2169.1428	2169.1556	316–334	RPFTQNLGLEELGIELDPK	41 (37)	

[1] To whom correspondence should be addressed (email mpm@mrc-mbu.cam.ac.uk).

Table S2 Identity of proteins containing thiols S-nitrosated and/or oxidized by MitoSNO

Protein spots were excised from 2D gels, digested with trypsin by the 'in-gel' cleavage method and analysed by MALDI–TOF-TOF MS. For peptide masses (MS data), MASCOT scores >59 (*Rattus* database) are significant ($P < 0.05$). For the MS/MS fragment masses (supporting tandem MS data) the values required for significance ($P < 0.05$) are reported in brackets after the MASCOT ion score. Amino acids are abbreviated using standard one character symbols, underlines indicate oxidized residues. Residue numbers correspond to the complete prtoein sequences found in the NCBI database. MM, molecular mass.

Candidate			MS data				Supporting tandem MS data			
NCBInr 'gi' accession	Protein name	MM (pI)	% Sequence coverage	Peptide matches at 25 p.p.m./supplied	MASCOT PMF score	Observed	Mass (MH^+) calculated	Residues	Sequence	MASCOT score ($P < 0.05$)
40538860	Mitochondrial aconitase	82462 (7.15)	38	28 of 42	463	1463.7299	1463.7489	412–424	SQFTITPGSEQIR	43 (38)
						1500.7908	1500.7693	522–534	FKLEAPDADELPR	67 (33)
						1601.8160	1601.7918	634–648	NAVTQEFGPVPDTAR	39 (33)
						1667.7926	1667.7660	657–671	WVVIGDENYGEGSSR	85 (33)
						1868.9332	1868.9137	69–84	IVYGHLDDPANQEIER	33 (33)
62945278	α-KGDH	111686 (6.00)	12	17 of 30	173	1402.6545	1402.6750	962–972	NQGYYDYVKPR	52 (29)
						2002.0024	2001.9988	82–101	NTNAGAPPGTAYQSPLSLSR	65 (32)
						929.4537	928.4654	908–914	VYYDLTR	25 (24)
25742763	78 kDa Glucose-regulated protein	72302 (5.07)	19	24 of 28	415	1566.7546	1566.7799	62–75	ITPSYVAFTPEGER	39 (33)
						1887.9493	1887.9712	166–182	VTHAVVTVPAYFNDAQR	49 (33)
						1933.9932	1934.0131	476–493	DNHLLGTFDLTGIPPAPR	75 (33)
						2148.9915	2148.9972	308–325	IEIESFFEGEDFSETLTR	52 (33)
6978435	Very long chain acyl-CoA dehydrogenase	66382 (8.10)	17	9 of 27	103	1316.7367	1316.7321	557–567	GIVNEQFLLQR	47 (34)
						2577.3167	2577.3306	138–162	ELGAFGLQVPSELGGLGLSNTQYAR	20 (34)
52138635	Electron-transferring flavoprotein dehydrogenase	64483 (6.47)	21	15 of 31	261	1291.6418	1291.6277	548–558	NLSIYDGPEQR	37 (38)
						1428.7814	1428.7706	344–356	HHPSIRPTLEGGK	42 (38)
						2113.1201	2113.1288	64–85	FAEEADVVIVGAGPAGLSAAIR	68 (33)
1850592	Carnitine palmitoyl transferase 2	71262 (6.43)	49	21 of 27	520	958.4824	958.4782	383–389	FFNEVFR	40 (33)
						1650.8552	1650.8850	168–182	AGLLEPEVFHLNPSK	77 (33)
						1807.9280	1807.9337	64–78	YLNAQKPLLDDSQFR	73 (33)
						2484.2603	2484.2293	275–296	YILSDSSPVPEFPVAYLTSENR	112 (33)
2392291	Enoyl-CoA hydratase chain A	28287 (6.41)	36	11 of 25	160	1311.6677	1311.6593	87–96	FLSHWDHITR	20 (37)
						2111.1326	2111.1244	129–149	AQFGQPEILLGTIPGAGGTQR	74 (37)
51948476	Complex III, core protein 1	49380 (5.22)	10	8 of 19	165	1580.7802	1580.7856	86–99	NNGAGYFLEHLAFK	78 (32)
						1646.8246	1646.8133	112–126	EVESIGAHLNAYSTR	37 (32)
14192933	ALDH2	54368 (5.69)	9	8 of 12	180	1470.7606	1470.7628	397–409	GYFIQPTVFGDVK	72 (39)
						1531.7502	1531.7428	162–174	TIPIDGDFFSYTR	27 (34)
						1775.8210	1775.8123	327–340	TFVQEDVYDEFVER	58 (34)
57527204	Electron-transferring flavoprotein α polypeptide	34929 (8.62)	31	12 of 25	437	1662.7885	1662.7976	188–203	APSSSSAGISEWLDQK	118 (38)
						1794.0237	1794.0265	86–101	GLLPEELTPLILETQK	72 (38)
						1812.9580	1812.9609	233–249	LLYDLADQLHAAVGASR	89 (38)
						1920.9028	1920.9127	250–268	AAVDAGFVPNDMQVGQTGK	73 (38)

Table S2 Continued

Candidate			MS data				Supporting tandem MS data			
NCBInr 'gi' accession	Protein name	MM (pI)	% Sequence coverage	Peptide matches at 25 p.p.m./supplied	MASCOT PMF score	Observed	Mass (MH^+) calculated	Residues	Sequence	MASCOT score ($P < 0.05$)
6978431	Long chain acyl-CoA dehydrogenase	44672 (6.26)	33	12 of 35	272	1250.5932	1250.6164	52–61	IFSSEHDIFR	77 (37)
						1406.7296	1406.7175	51–61	RIFSSEHDIFR	33 (37)
						1540.7471	1540.7278	255–267	AQDTAELFFEDVR	97 (37)
						1673.7982	1673.7992	280–292	GFYYLMQELPQER	41 (38)
20304123	3-Mercaptopyruvate sulfurtransferase	32809 (5.88)	28	14 of 20	277	1221.6252	1221.6335	283–293	AQPEHVISQGR	39 (39)
						1358.6824	1358.6852	53–64	HIPGAAFFDIDR	50 (39)
						1425.6897	1425.6968	165–176	THEDILENLDAR	52 (39)
						1599.7974	1599.8027	119–133	AFGHHSVSLLDGGFR	38 (39)
149036390	Mitofilin	83484 (6.18)	27	25 of 35	391	1271.5773	1271.5790	486–495	FEFEQDLSEK	42 (32)
						1287.6494	1287.6328	496–505	LSEQELEFHR	38 (32)
						1823.8929	1823.8882	527–543	GIEQAVQSHAVAEEEAR	101 (32)
18426858	Succinate dehydrogenase, subunit A flavoprotein	68004 (6.17)	29	22 of 45	478	1122.5885	1122.5902	243–253	NTIIATGGYGR	39 (39)
						1318.7384	1318.7365	629–639	VTLDYRPVIDK	42 (39)
						1329.6759	1329.6757	305–317	GEGGILINSQGER	76 (39)
						1354.7200	1354.7226	188–199	TGHSLLHTLYGR	57 (39)
						1473.8397	1473.8424	444–457	LGANSLLDLVVFGR	84 (39)
						2167.1306	2167.1407	354–371	DHVYLQLHHLPPEQLATR	53 (39)
62079055	Isocitrate dehydrogenase ($NADP^+$) mitochondrial	46640 (8.49)	20	11 of 46	96	903.4569	903.4472	283–288	IWYEHR	20 (37)
						976.5684	976.5575	141–149	NILGGTVFR	38 (37)
11968090	Short-chain acyl-CoA dehydrogenase	42187 (6.38)	15	7 of 18	73	1260.6730	1260.6616	316–327	LADMALALESAR	42 (39)
3915779	Myosin heavy chain 6	223488 (5.68)	27	30 of 39	432	1030.5499	1030.5891	1240–1248	EALISQLTR	36 (37)
						1081.4875	1081.5273	1214–1222	SLNDFTTQR	57 (37)
						1090.5449	1090.5891	1506–1514	AQLEFNQIK	41 (37)
						1151.5863	1151.6280	1272–1282	NALAHALQSAR	72 (37)
						1238.5234	1238.5648	1196–1205	TLEDQANEYR	64 (37)
						1428.7229	1428.7693	1623–1634	NTLLQAELEELR	90 (37)

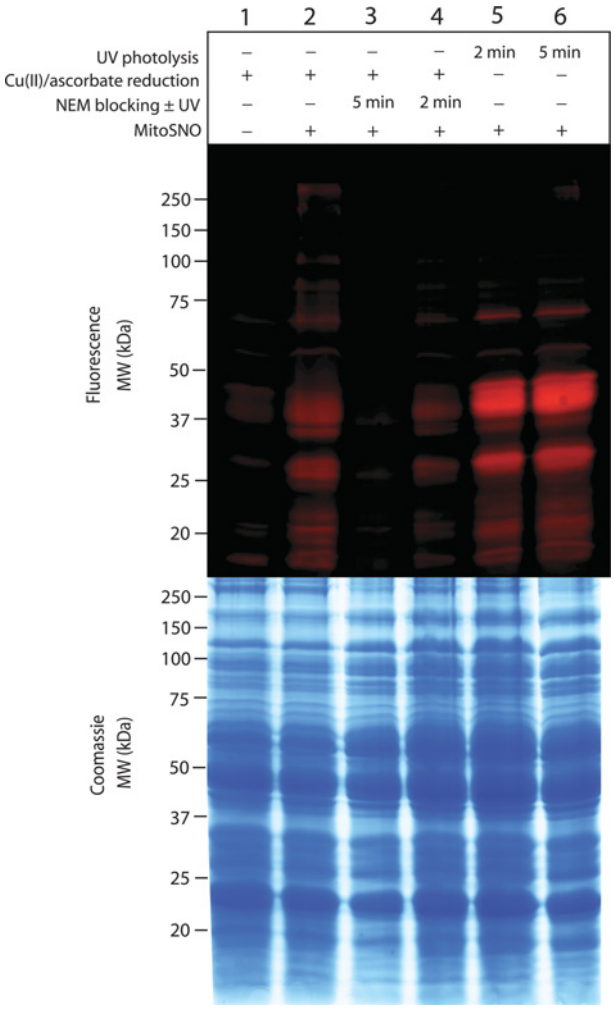

Figure S1 UV photolysis of S-nitrosated mitochondrial protein thiols

To further ensure the specificity of PrSNO reduction by Cu(II) and ascorbate and labelling by fluorescent maleimide dyes, UV photolysis of PrSNOs was employed. As anticipated, treatment with MitoSNO followed by NEM blocking of free protein thiols and reduction of PrSNOs by Cu(II) and ascorbate in the presence of a fluorescent maleimide dye (lane 2) resulted in significant labelling when compared with the no MitoSNO control (lane 1). UV photolysis of PrSNOs following MitoSNO treatment but before NEM blocking of free thiols resulted in a time-dependent loss of the fluorescent signal (lanes 3 and 4). Alternatively, employing UV photolysis instead of Cu(II) and ascorbate reduction of PrSNOs following NEM blocking (lanes 5 and 6) resulted in a very similar fluorescent signal to the reduction conditions used in the DIGE analysis (lane 2).

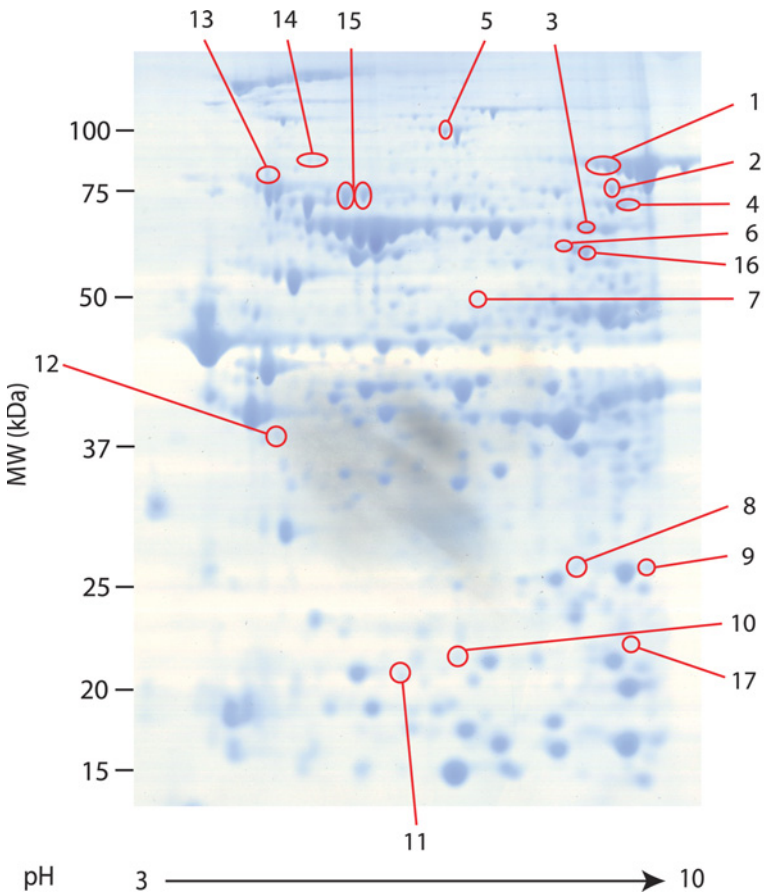

1. Aconitase
2. Electron transferring flavoprotein, dehydrogenase
3. Carnitine palmitoyl transferase 2
4. Very long chain acyl-CoA dehydrogenase
5. α-ketoglutarate dehydrogenase
6. succinate dehydrogenase, subunit A flavoprotein
7. Mitochondrial aldehyde dehydrogenase
8. Eletron transferring flavoprotein, alpha polypeptide
9. Long chain acyl-CoA dehydrogenase
10. Enoyl-CoA hydratase
11. 3-mercaptopyruvate sulfurtransferase
12. Complex III, core protein 1
13. 78 kDa glucose regulated protein
14. Myosin heavy chain 6
15. Mitofilin
16. Isocitrate dehydrogenase (NADP+)
17. Short chain acyl-CoA dehydrogenase

Figure S2 A typical Coomassie Blue-stained gel

The red circles indicate the protein spots that showed significant changes in the SNO-DIGE and/or Redox-DIGE analyses and were analysed by MS. The identities of the proteins are listed beside the gel image. For detailed MALDI–TOF-TOF data, see Table S2. MW, molecular mass.

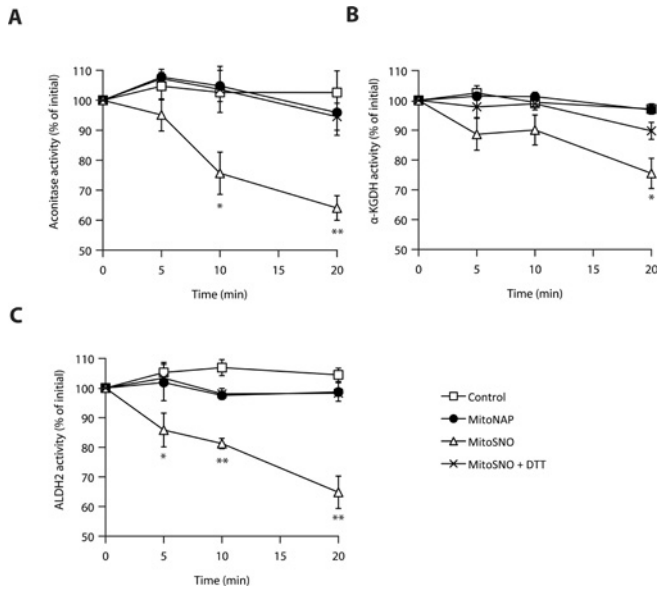

Figure S3 Additional functional characterization of S-nitrosation by MitoSNO

Metabolic enzymes found to be S-nitrosated and inhibited due to MitoSNO action were tested for reversibility with DTT and effects due to the mitochondrial targeting moeity. (**A**) Mitochondrial aconitase activity was found to decrease, beginning 5 min following MitoSNO treatment and showing significant inhibition beyond 10 min when compared with vehicle treated and MitoNAP-treated controls. Addition of DTT to reduce modifications following treatment with MitoSNO completely reversed the inhibitory effect. (**B**) α-KGDH activity was also inhibited by MitoSNO action, causing significant inhibition 20 min following MitoSNO addition. The inhibitory effect of MitoSNO was reversed with DTT. (**C**) MitoSNO significantly inhibited mitochondrial ALDH2 5 min following its addition and onwards, and the inhibitory effect was completely reversed by DTT. Error bars show means $\pm$ S.E.M.; $^{*}P < 0.05$; $^{**}P < 0.01$ by Student's *t* test.

Received 23 April 2010/9 June 2010; accepted 10 June 2010
Published as BJ Immediate Publication 10 June 2010, doi:10.1042/BJ20100633

BJ www.biochemj.org

Biochem. J. (2010) **430**, 49–59 (Printed in Great Britain) doi:10.1042/BJ20100633

SUPPLEMENTARY ONLINE DATA

Identification of S-nitrosated mitochondrial proteins by *S*-nitrosothiol difference in gel electrophoresis (SNO-DIGE): implications for the regulation of mitochondrial function by reversible S-nitrosation

Edward T. CHOUCHANI*, Thomas R. HURD*, Sergiy M. NADTOCHIY†, Paul S. BROOKES†, Ian M. FEARNLEY*, Kathryn S. LILLEY‡, Robin A. J. SMITH§ and Michael P. MURPHY*[1]

*MRC Mitochondrial Biology Unit, Hills Road, Cambridge CB2 0XY, U.K., †Department of Anesthesiology, University of Rochester Medical Center, 601 Elmwood Avenue, Rochester, NY 14642, U.S.A., ‡Department of Biochemistry, Cambridge System Biology Centre, University of Cambridge, Cambridge CB2 1GA, U.K., and §Department of Chemistry, University of Otago, P.O. Box 56, Dunedin 9054, New Zealand

Table S1 Identity of thiol proteins containing occluded thiols determined by SNO-DIGE and Redox-DIGE

Protein spots were excised from 2D gels, digested with trypsin by the 'in-gel' cleavage method and analysed by MALDI–TOF-TOF MS. For peptide ion masses searched (MS data), MASCOT scores>59 (*Rattus* database) are significant ($P<0.05$). For the tandem MS fragment masses (supporting tandem MS data), the values required for significance ($P<0.05$) are reported in brackets after the MASCOT ion score. Amino acids are abbreviated using standard one character symbols. Residue numbers correspond to the complete protein sequences found in the NCBI database. The established nature of the occluded thiols for each candidate is included. MM, molecular mass.

Candidate			MS data				Supporting tandem MS data				
NCBInr 'gi' accession	Protein name	MM (pI)	% Sequence coverage	Peptide matches at 25 p.p.m./ supplied	MASCOT score	Observed	Mass (MH^+) calculated	Residues	Sequence	MASCOT score ($P < 0.05$)	Thiols
58865384	Complex I 49 kDa subunit	49243 (5.95)	29	18 of 45	355	934.5278	934.5363	172–179	VLFGEITR	50 (38)	Fe-S
						1047.6228	1047.6315	158–166	LLNIQPPPR	43 (38)	
						2228.1182	2228.0512	305–323	TQPYDVYDQVEFDVPIGSR	111 (38)	
51092268	Complex I 24 kDa subuit	23933 (5.07)	32	11 of 18	320	1244.6405	1244.6375	199–208	DIEEIIDELR	64 (29)	Fe-S
						1336.7994	1336.7953	75–87	AAAVLPVLDLAQR	63 (29)	
						2398.0083	2398.0112	42–61	DTPENNPDTPFDFTPENYER	126 (29)	
125313	Mitochondrial creatine kinase	43144 (7.78)	30	14 of 45	348	1390.6908	1390.7008	47–58	LFPPSADYPDLR	57 (38)	Exposed
						2109.0044	2109.0101	285–305	GTGGVDTAAVADVYDISNIDR	121 (38)	
						1673.8197	1673.8288	258–270	TFLIWINEEDHTR	59 (38)	
40786469	Dihydrolipoamide dehydrogenase	50089 (6.51)	20	12 of 41	217	1127.6536	1127.6578	133–143	ALTGGIAHLFK	42 (37)	Exposed
						1737.8724	1737.8825	90–104	ALLNNSHYYHLAHGK	73 (37)	
						2169.1428	2169.1556	316–334	RPFTQNLGLEELGIELDPK	41 (37)	

[1] To whom correspondence should be addressed (email mpm@mrc-mbu.cam.ac.uk).

Table S2 Identity of proteins containing thiols S-nitrosated and/or oxidized by MitoSNO

Protein spots were excised from 2D gels, digested with trypsin by the 'in-gel' cleavage method and analysed by MALDI–TOF-TOF MS. For peptide masses (MS data), MASCOT scores >59 (*Rattus* database) are significant ($P < 0.05$). For the MS/MS fragment masses (supporting tandem MS data) the values required for significance ($P < 0.05$) are reported in brackets after the MASCOT ion score. Amino acids are abbreviated using standard one character symbols, underlines indicate oxidized residues. Residue numbers correspond to the complete prtoein sequences found in the NCBI database. MM, molecular mass.

Candidate			MS data				Supporting tandem MS data			
NCBInr 'gi' accession	Protein name	MM (pI)	% Sequence coverage	Peptide matches at 25 p.p.m./supplied	MASCOT PMF score	Observed	Mass (MH^+) calculated	Residues	Sequence	MASCOT score ($P < 0.05$)
40538860	Mitochondrial aconitase	82462 (7.15)	38	28 of 42	463	1463.7299	1463.7489	412–424	SQFTITPGSEQIR	43 (38)
						1500.7908	1500.7693	522–534	FKLEAPDADELPR	67 (33)
						1601.8160	1601.7918	634–648	NAVTQEFGPVPDTAR	39 (33)
						1667.7926	1667.7660	657–671	WVVIGDENYGEGSSR	85 (33)
						1868.9332	1868.9137	69–84	IVYGHLDDPANQEIER	33 (33)
62945278	α-KGDH	111686 (6.00)	12	17 of 30	173	1402.6545	1402.6750	962–972	NQGYYDYVKPR	52 (29)
						2002.0024	2001.9988	82–101	NTNAGAPPGTAYQSPLSLSR	65 (32)
						929.4537	928.4654	908–914	VYYDLTR	25 (24)
25742763	78 kDa Glucose-regulated protein	72302 (5.07)	19	24 of 28	415	1566.7546	1566.7799	62–75	ITPSYVAFTPEGER	39 (33)
						1887.9493	1887.9712	166–182	VTHAVVTVPAYFNDAQR	49 (33)
						1933.9932	1934.0131	476–493	DNHLLGTFDLTGIPPAPR	75 (33)
						2148.9915	2148.9972	308–325	IEIESFFEGEDFSETLTR	52 (33)
6978435	Very long chain acyl-CoA dehydrogenase	66382 (8.10)	17	9 of 27	103	1316.7367	1316.7321	557–567	GIVNEQFLLQR	47 (34)
						2577.3167	2577.3306	138–162	ELGAFGLQVPSELGGLGLSNTQYAR	20 (34)
52138635	Electron-transferring flavoprotein dehydrogenase	64483 (6.47)	21	15 of 31	261	1291.6418	1291.6277	548–558	NLSIYDGPEQR	37 (38)
						1428.7814	1428.7706	344–356	HHPSIRPTLEGGK	42 (38)
						2113.1201	2113.1288	64–85	FAEEADVVIVGAGPAGLSAAIR	68 (33)
1850592	Carnitine palmitoyl transferase 2	71262 (6.43)	49	21 of 27	520	958.4824	958.4782	383–389	FFNEVFR	40 (33)
						1650.8552	1650.8850	168–182	AGLLEPEVFHLNPSK	77 (33)
						1807.9280	1807.9337	64–78	YLNAQKPLLDDSQFR	73 (33)
						2484.2603	2484.2293	275–296	YILSDSSPVPEFPVAYLTSENR	112 (33)
2392291	Enoyl-CoA hydratase chain A	28287 (6.41)	36	11 of 25	160	1311.6677	1311.6593	87–96	FLSHWDHITR	20 (37)
						2111.1326	2111.1244	129–149	AQFGQPEILLGTIPGAGGTQR	74 (37)
51948476	Complex III, core protein 1	49380 (5.22)	10	8 of 19	165	1580.7802	1580.7856	86–99	NNGAGYFLEHLAFK	78 (32)
						1646.8246	1646.8133	112–126	EVESIGAHLNAYSTR	37 (32)
14192933	ALDH2	54368 (5.69)	9	8 of 12	180	1470.7606	1470.7628	397–409	GYFIQPTVFGDVK	72 (39)
						1531.7502	1531.7428	162–174	TIPIDGDFFSYTR	27 (34)
						1775.8210	1775.8123	327–340	TFVQEDVYDEFVER	58 (34)
57527204	Electron-transferring flavoprotein α polypeptide	34929 (8.62)	31	12 of 25	437	1662.7885	1662.7976	188–203	APSSSSAGISEWLDQK	118 (38)
						1794.0237	1794.0265	86–101	GLLPEELTPLILETQK	72 (38)
						1812.9580	1812.9609	233–249	LLYDLADQLHAAVGASR	89 (38)
						1920.9028	1920.9127	250–268	AAVDAGFVPNDMQVGQTGK	73 (38)

Table S2 Continued

Candidate			MS data				Supporting tandem MS data			
NCBInr 'gi' accession	Protein name	MM (pI)	% Sequence coverage	Peptide matches at 25 p.p.m./supplied	MASCOT PMF score	Observed	Mass (MH^+) calculated	Residues	Sequence	MASCOT score ($P < 0.05$)
6978431	Long chain acyl-CoA dehydrogenase	44672 (6.26)	33	12 of 35	272	1250.5932	1250.6164	52–61	IFSSEHDIFR	77 (37)
						1406.7296	1406.7175	51–61	RIFSSEHDIFR	33 (37)
						1540.7471	1540.7278	255–267	AQDTAELFFEDVR	97 (37)
						1673.7982	1673.7992	280–292	GFYYLMQELPQER	41 (38)
20304123	3-Mercaptopyruvate sulfurtransferase	32809 (5.88)	28	14 of 20	277	1221.6252	1221.6335	283–293	AQPEHVISQGR	39 (39)
						1358.6824	1358.6852	53–64	HIPGAAFFDIDR	50 (39)
						1425.6897	1425.6968	165–176	THEDILENLDAR	52 (39)
						1599.7974	1599.8027	119–133	AFGHHSVSLLDGGFR	38 (39)
149036390	Mitofilin	83484 (6.18)	27	25 of 35	391	1271.5773	1271.5790	486–495	FEFEQDLSEK	42 (32)
						1287.6494	1287.6328	496–505	LSEQELEFHR	38 (32)
						1823.8929	1823.8882	527–543	GIEQAVQSHAVAEEEAR	101 (32)
18426858	Succinate dehydrogenase, subunit A flavoprotein	68004 (6.17)	29	22 of 45	478	1122.5885	1122.5902	243–253	NTIIATGGYGR	39 (39)
						1318.7384	1318.7365	629–639	VTLDYRPVIDK	42 (39)
						1329.6759	1329.6757	305–317	GEGGILINSQGER	76 (39)
						1354.7200	1354.7226	188–199	TGHSLLHTLYGR	57 (39)
						1473.8397	1473.8424	444–457	LGANSLLDLVVFGR	84 (39)
						2167.1306	2167.1407	354–371	DHVYLQLHHLPPEQLATR	53 (39)
62079055	Isocitrate dehydrogenase ($NADP^+$) mitochondrial	46640 (8.49)	20	11 of 46	96	903.4569	903.4472	283–288	IWYEHR	20 (37)
						976.5684	976.5575	141–149	NILGGTVFR	38 (37)
11968090	Short-chain acyl-CoA dehydrogenase	42187 (6.38)	15	7 of 18	73	1260.6730	1260.6616	316–327	LADMALALESAR	42 (39)
3915779	Myosin heavy chain 6	223488 (5.68)	27	30 of 39	432	1030.5499	1030.5891	1240–1248	EALISQLTR	36 (37)
						1081.4875	1081.5273	1214–1222	SLNDFTTQR	57 (37)
						1090.5449	1090.5891	1506–1514	AQLEFNQIK	41 (37)
						1151.5863	1151.6280	1272–1282	NALAHALQSAR	72 (37)
						1238.5234	1238.5648	1196–1205	TLEDQANEYR	64 (37)
						1428.7229	1428.7693	1623–1634	NTLLQAELEELR	90 (37)

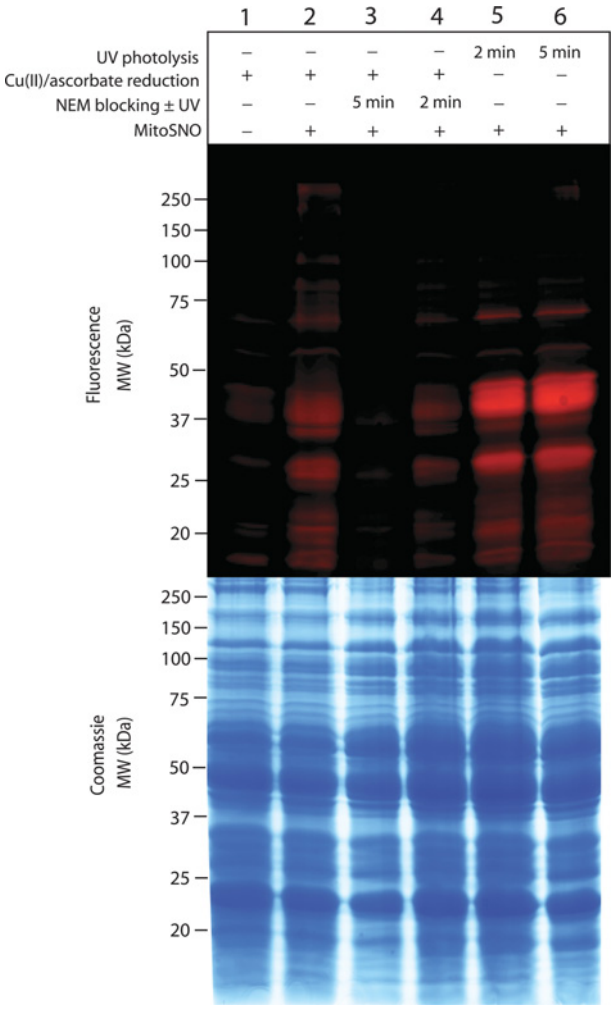

Figure S1 UV photolysis of S-nitrosated mitochondrial protein thiols

To further ensure the specificity of PrSNO reduction by Cu(II) and ascorbate and labelling by fluorescent maleimide dyes, UV photolysis of PrSNOs was employed. As anticipated, treatment with MitoSNO followed by NEM blocking of free protein thiols and reduction of PrSNOs by Cu(II) and ascorbate in the presence of a fluorescent maleimide dye (lane 2) resulted in significant labelling when compared with the no MitoSNO control (lane 1). UV photolysis of PrSNOs following MitoSNO treatment but before NEM blocking of free thiols resulted in a time-dependent loss of the fluorescent signal (lanes 3 and 4). Alternatively, employing UV photolysis instead of Cu(II) and ascorbate reduction of PrSNOs following NEM blocking (lanes 5 and 6) resulted in a very similar fluorescent signal to the reduction conditions used in the DIGE analysis (lane 2).

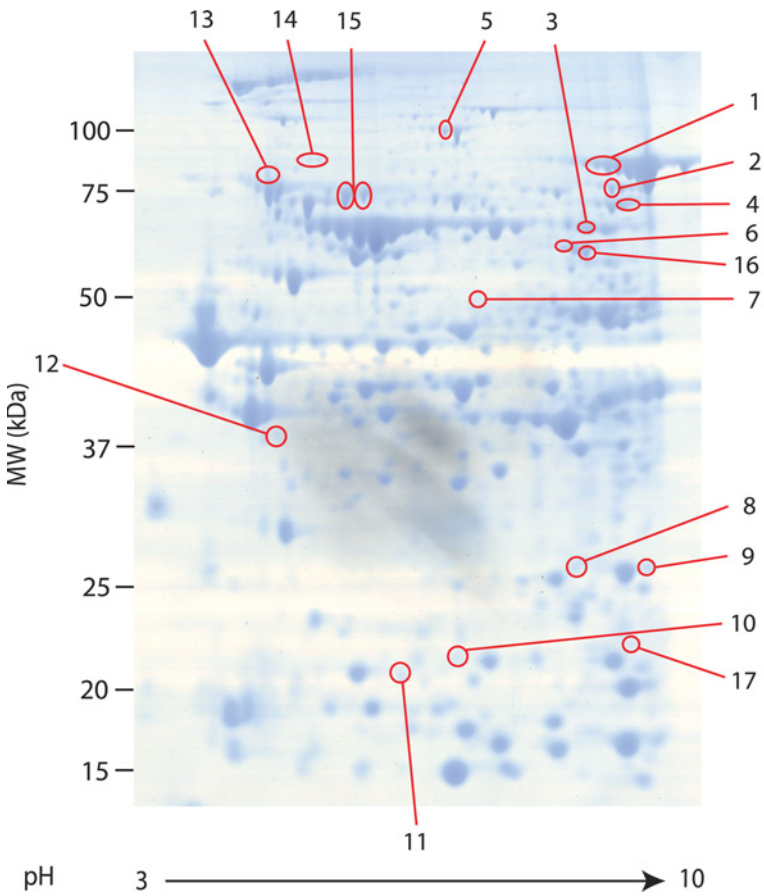

1. Aconitase
2. Electron transferring flavoprotein, dehydrogenase
3. Carnitine palmitoyl transferase 2
4. Very long chain acyl-CoA dehydrogenase
5. α-ketoglutarate dehydrogenase
6. succinate dehydrogenase, subunit A flavoprotein
7. Mitochondrial aldehyde dehydrogenase
8. Eletron transferring flavoprotein, alpha polypeptide
9. Long chain acyl-CoA dehydrogenase
10. Enoyl-CoA hydratase
11. 3-mercaptopyruvate sulfurtransferase
12. Complex III, core protein 1
13. 78 kDa glucose regulated protein
14. Myosin heavy chain 6
15. Mitofilin
16. Isocitrate dehydrogenase (NADP+)
17. Short chain acyl-CoA dehydrogenase

Figure S2 A typical Coomassie Blue-stained gel

The red circles indicate the protein spots that showed significant changes in the SNO-DIGE and/or Redox-DIGE analyses and were analysed by MS. The identities of the proteins are listed beside the gel image. For detailed MALDI–TOF-TOF data, see Table S2. MW, molecular mass.

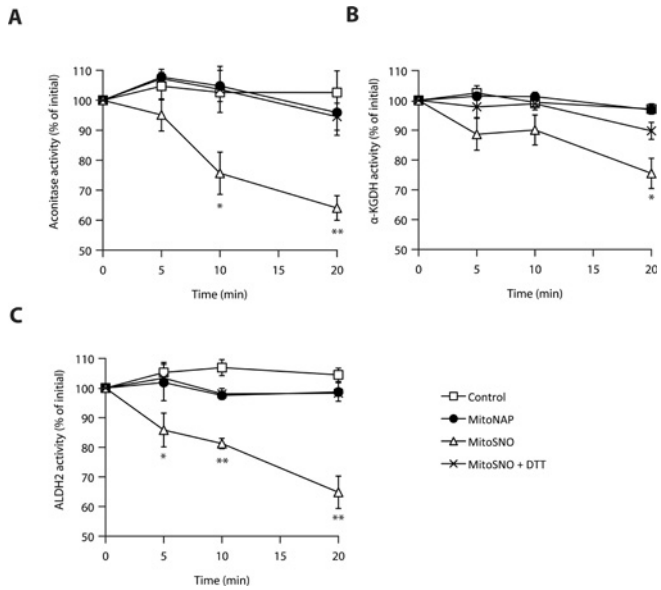

Figure S3 Additional functional characterization of S-nitrosation by MitoSNO

Metabolic enzymes found to be S-nitrosated and inhibited due to MitoSNO action were tested for reversibility with DTT and effects due to the mitochondrial targeting moeity. (**A**) Mitochondrial aconitase activity was found to decrease, beginning 5 min following MitoSNO treatment and showing significant inhibition beyond 10 min when compared with vehicle treated and MitoNAP-treated controls. Addition of DTT to reduce modifications following treatment with MitoSNO completely reversed the inhibitory effect. (**B**) α-KGDH activity was also inhibited by MitoSNO action, causing significant inhibition 20 min following MitoSNO addition. The inhibitory effect of MitoSNO was reversed with DTT. (**C**) MitoSNO significantly inhibited mitochondrial ALDH2 5 min following its addition and onwards, and the inhibitory effect was completely reversed by DTT. Error bars show means $\pm$ S.E.M.; $^{*}P < 0.05$; $^{**}P < 0.01$ by Student's *t* test.

Received 23 April 2010/9 June 2010; accepted 10 June 2010
Published as BJ Immediate Publication 10 June 2010, doi:10.1042/BJ20100633